國 立 交 通 大 學

電信工程研究所

碩 士 論 文

合作式定位之低維度最小方差演算法

Dimension-Reduced Least-Squares Algorithms for Cooperative Localization

研究生：李冠杰

指導教授：謝世福 教授

中 華 民 國 一百零一 年 七 月

合作式定位之低維度最小方差演算法

Dimension-Reduced Least-Squares Algorithms for Cooperative Localization

研 究 生：李冠杰　　Student：K.C. Lee

指導教授：謝世福　　Advisor：S. F. Hsieh

國 立 交 通 大 學

電信工程研究所

碩 士 論 文

A Thesis

Submitted to Institute of Electrical Engineering

College of Electrical and Computer Science

National Chiao Tung University

In Partial Fulfillment of the Requirements

For the Degree of

Master

In

Communication Engineering

July 2012

Hsinchu, Taiwan, Republic of China

中華民國一百零一年七月

合作式定位之低維度最小方差演算法

學生:李冠杰　　指導教授:謝世福

國立交通大學電信工程研究所

中文摘要

隨著無線通訊的發展，定位的研究已成為重要的議題。近年來，藉由待測物之間彼此相互通訊的合作式定位更是目前發展的重點。在合作式定位系統中，多個待測目標之間額外的合作量測可以有效提升其定位的精準度；但由於待測目標的增加，因此演算法的複雜度相較於傳統定位法更是困難許多。在諸多演算法中，高斯-牛頓法被廣泛的應用在定位的問題中，效能也與 Cramer-Rao Lower Bound (CRLB) 相當；然而其牽涉到反矩陣的運算，使得伴隨而來的複雜度相當高。我們試著藉由降低矩陣的維度使反矩陣的運算量降低，進而達到降低複雜度的目標。在論文中，我們設定一個待測物為目標待測物，並試著尋找其餘附屬待測物與目標待測物之間的位置關係，藉此來達到降低運算度的目的，並維持其定位準確度。因此，我們提出了聯合式、平行式與序列式三種預先線性化的方法使附屬待測物的位置座標轉化成目標待測物的線性函式。接著再利用此線性函式使原來的多待測物問題降階成一個目標待測物的估計問題並利用低維度高斯-牛頓法來估計。其中平行式與序列式的演算法運算複雜度順利的被簡化。另外，基於目標待測物的位置估計的影響，我們更進一步提出目標待測物的選擇機制，進而增進定位的效能；另一方面，根據待測物的不確定性，我們對於權重也做了額外的補償。電腦模擬驗證了目標待測物的選擇機制及權重補償能夠提高定位準確度；另外也比較了高斯-牛頓法與我們提出的預先線性法，證明在不失定位準度的情況下，減少了運算複雜度。

Dimension-Reduced Least-Squares Algorithms for Cooperative Localization

Student: K. C. Lee Advisor：S. F. Hsieh

Department of Communication Engineering

National Chiao Tung University

Abstract

Cooperative localization has received extensive interest from the robotic, optimization, and wireless communication. In addition to the range measurements from the mobile and BSs with known position, the extra information among mobiles is added to improve the accuracy of position in cooperative localization. The Gauss-Newton (GN) method can be used to solve the cooperative positioning problem with good performance, but its computational complexity is quite high due to the matrix inversion. However, if the dimension is reduced, the complexity of algorithm is reduced as well. In this thesis, a target mobile is selected as reference mobile, we want to find the relationship between auxiliary mobiles and the target mobile. Therefore, we propose three pre-linear methods, joint, parallel and sequential methods, which can reduce dimension of the unknown parameters by searching the linear mapping relations from auxiliary mobiles to target mobile. With the pre-linear mapping function, the dimension-reduced GN method of target mobile is derived based on the conventional GN method. The total computational cost can be reduced greatly in parallel and sequential methods. Moreover, the choice of target mobile and compensation of inaccurate mobiles are discussed to enhance the localization accuracy. Simulations validate the enhancement of accuracy. In addition, we also compare performance of RMSE and total computation cost for low-complexity pre-linear methods with GN method.

Acknowledgements

碩士班的日子酸甜苦辣，起初對於做研究沒有明確的方向，非常感謝謝世福老師的提點，讓我在研究中建立起正確的思考邏輯，另外在遇到的瓶頸時適時的引導，讓我能夠以更廣的角度看問題，我想這對我是最大的收穫。另外，也要感謝實驗室的學長姊與同學在我困惑之際給我及時的鼓勵，使碩士生活的壓力減輕許多。最後，也要感謝家人的支持，能夠讓我無後顧之憂的完成學業。

Table of Contents

List of Figures

List of Tables

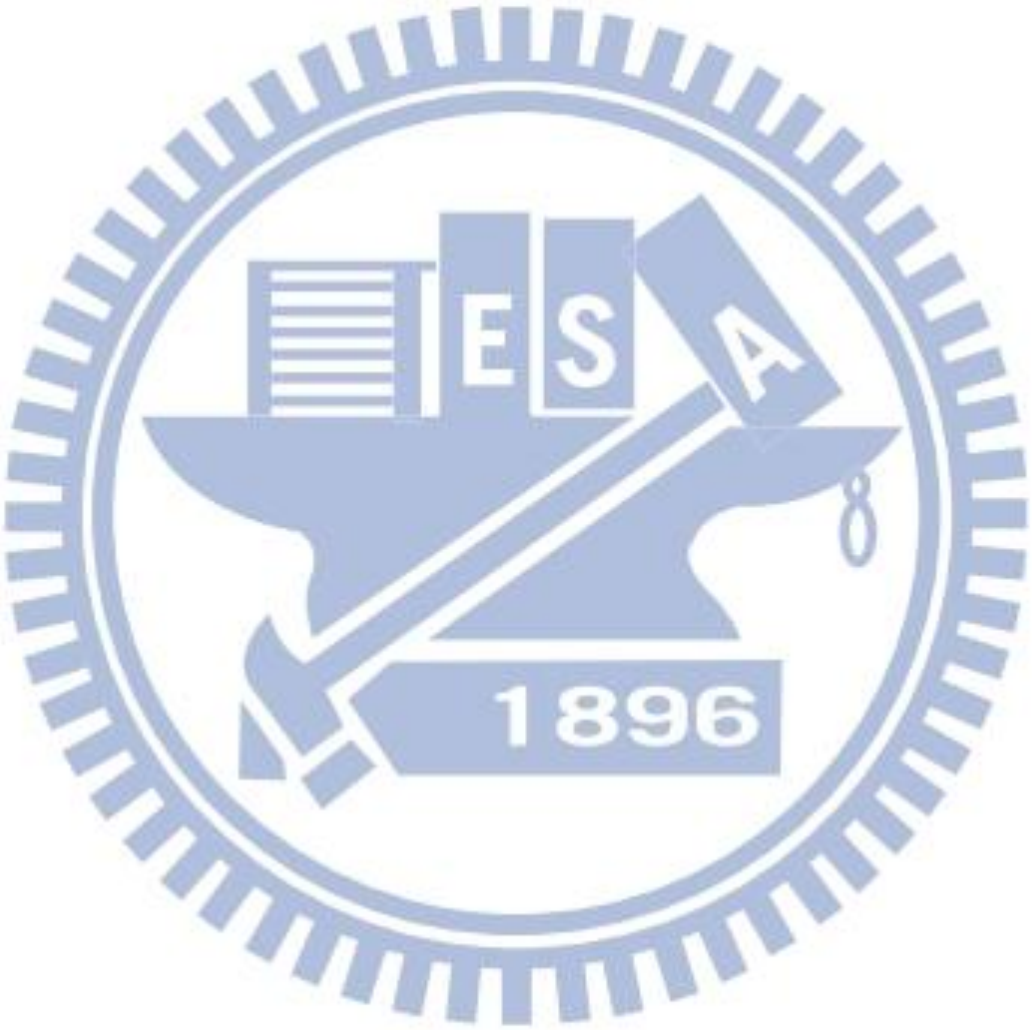

Chapter 1
Introduction

In recent years, positioning technology has attracted attention and developed rapidly [1]. It finds applications in military, commercial, emergency search and rescue. The most localization systems estimate the unknown position coordinates based on the information between the unknown position node and base stations (BSs) with known positions. The typical techniques of localization include measurements of time-of arrival (TOA) [2], time-different-of-arrival (TDOA) [3], angle-of-arrival (AOA) [4] and received signal strength (RSS) [5], hybrid TDOA/AOA and other mixture method [6]. In this thesis, we consider the TOA localization technique. Besides, the measurements may suffer from non-line-of-sight (NLOS) effect, [7] proposed an effective technique in NLOS environment by linearizing the inequalities of range models.

It is a crucial estimation problem that the unknown position coordinates are nonlinear because of the range equations. Nonlinear least-squares (NLS) estimator such as the Newton method [8], the Gauss-Newton (GN) method [9] can be used to solve the problem. These nonlinear iterative methods provide an estimator with high accuracy which is close to the Cramer-Rao Lower Bound (CRLB) under moderate measurement error. However, these iterative methods need highly computation costs and an initial guess of the unknown position is needed to start the iteration; the poor initial guess may degrade the performance of localization and the convergence rate. Another low cost method that attracts a lot of research interest is the Linear Least-Squares (LLS) method. [10-12] linearize the nonlinear range function and give a closed form solution. The advantage of the LLS method is its simplicity, but the obtained solution is suboptimal since the linear approximation. [13] proposed a one dimension iterative (1D-I) method which combined the LLS and GN method, the original

three-dimensions estimation can be reduced to one dimension by mapping x-axis and y-axis coordinates to the fixed linear function of z-axis coordinate, then solve the remaining one-dimension parameter by GN method iteratively.

In cooperative localization system, Mobiles exchange the information mutually can improve the accuracy of location estimation. It is more difficult than conventional localization since the additional measurements between mobiles are involved to enhance the accuracy. [14] devised subspace approach to solve the problem. In NLOS scenario, [15] presented a location verification protocol among cooperative neighboring vehicles to overcome NLOS condition.

Different from conventional localization, cooperative localization algorithm is more complicate by the increasing of unknown positions of mobiles. To simplify the existed algorithm, we extend the thought of 1D-I method of [13] in cooperative localization. In this thesis, we propose three pre-linear methods which lower the unknown positions coordinates by pre-linearizing the relation between mobiles, joint, parallel and sequential method. The measurements between mobiles are additionally useful information to locate the positions of mobiles in cooperative localization. For the reason, we select a mobile as target mobile, and the proposed pre-linear methods concern about the linear relationship from target mobile to auxiliary mobiles. Then, the dimension-reduced GN method of target mobile is used to estimate the positions of target mobile by using the information of pre-linear mapping function. Note that our research differs from [13] that the mapping we proposed is updated by iteration while the mapping in [13] is fixed. The detailed description will be given in Chapter 3. Compared with traditional GN method, the computation cost is reduced successfully in parallel and sequential methods with good location accuracy. On the other hand, the reliability of measurements between mobiles is an important issue; the uncertain positions of virtual BSs or the harsh environment between mobiles may degrade the accuracy. The weighting compensation of uncertain positions of mobiles and the mobile selection scheme are helpful to improve the accuracy of localization.

This thesis is organized as follow. In Chapter 2, the localization model is introduced first. Then, Least-squares algorithm including GN method which applied in our method is introduced. Three pre-linear methods are proposed and the dimension-reduced GN method is derived in Chapter 3. Chapter 3 also compares the total costs of proposed methods and GN method and discusses the issue of weighting compensation and mobile selection. Computer simulations will evaluate the Root Mean Square Error (RMSE) between pre-linear methods and GN method. Finally, we give a conclusion and future work in Chapter 6.

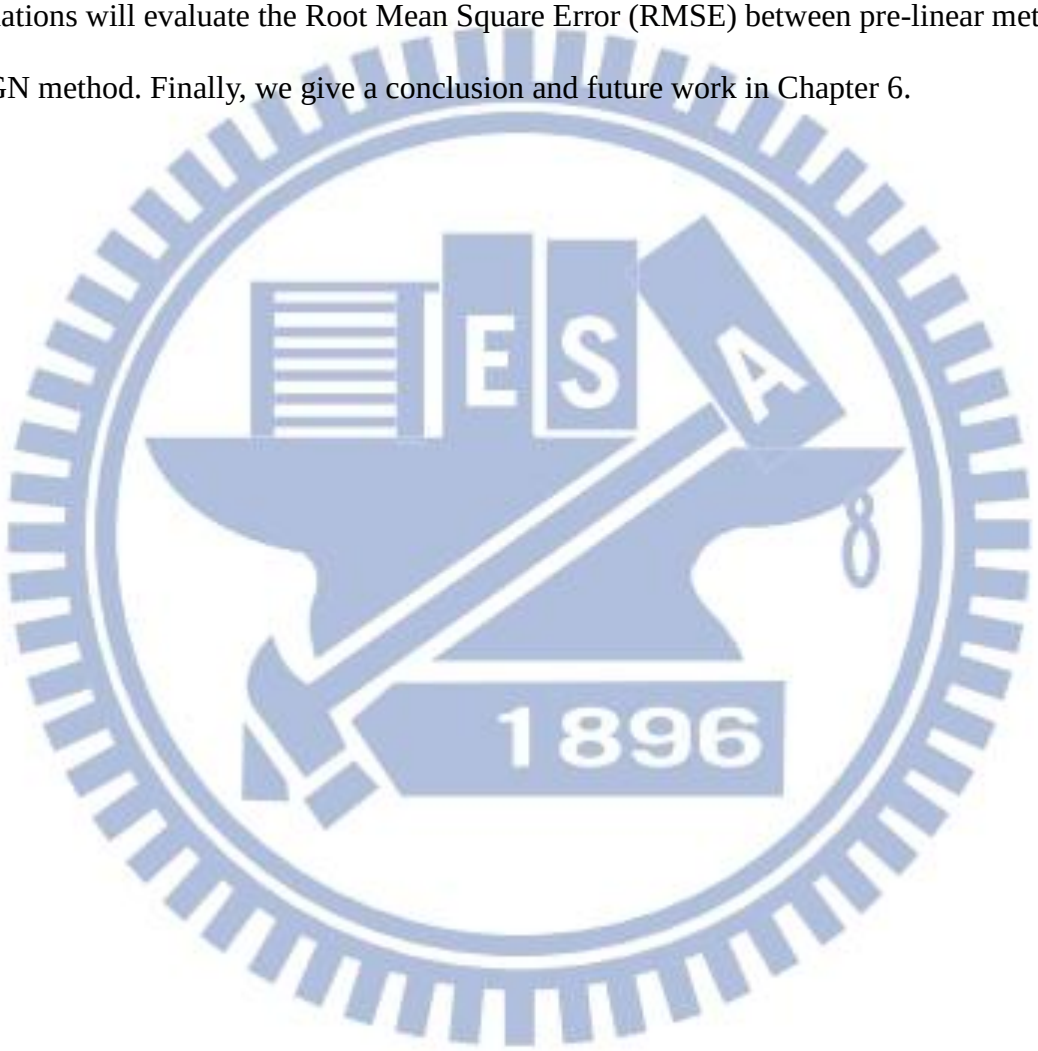

Chapter 2
Localization System

The localization estimation can be done by the measured data between mobiles and BSs. The estimation is usually done using iterative algorithms which solve nonlinear least-square (NLS) problem. The GN method is widely chosen to solve the nonlinear localization problem iteratively by means of linear interference. The performance of Mean Square Error (MSE) is known as well as the CRLB [1]. However, the computations of NLS estimator in each-iteration and the total load are quite heavy especially when a large number of iteration is required to converge. [10-12] proposed linear least-square (LLS) method to obtain the closed form solution. The transformed least-squares iterative method has been proposed recently in [13] which can reduce the complexity efficiently. In this chapter, Section 2.1 introduces the system model. LSE estimator and the CRLB are introduced in Section 2.2.

2.1 System Model

Figure 2.1 shows a basic localization system. There are *M* unknown positions of mobiles and *N* base stations with known positions. (x_i, y_i, z_i) and $(x_{\bar{j}}, y_{\bar{j}}, z_{\bar{j}})$ are coordinates of mobile *i* and BS $\bar{j}$, where $1 \le i \le M, 1 \le \bar{j} \le N$. Each mobile communicates with BSs independently and mobiles can exchange the information from received signal with each others. In this Chapter, we only concern measurements between mobiles and BSs, cooperative localization will be introduced in next Chapter.

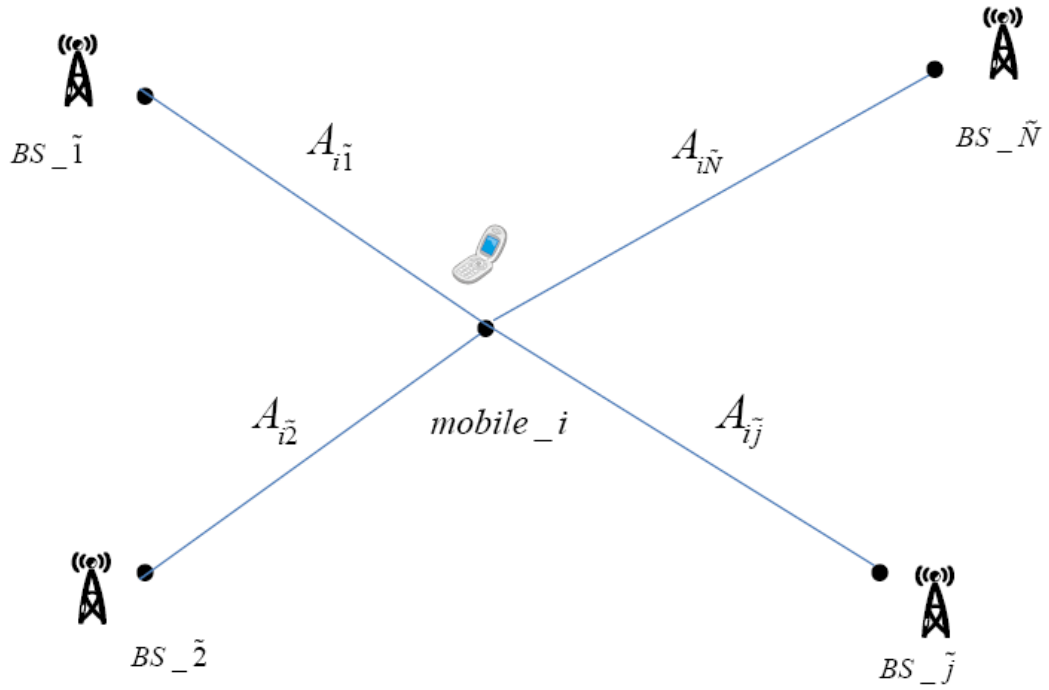

Figure 2.1 A basic localization system

In TOA scenario, measured distance *d* from mobiles to BSs can be calculated by multiplying the propagation time and the signal propagation speed. With TOA measurement from mobile *i* and BS *j*, we have measured distance modeled as

$$d_{i\tilde{j}} = A_{i\tilde{j}} + n_{i\tilde{j}}, \tilde{j} = 1,2,..,N \qquad (2.1)$$

where $A_{i\tilde{j}}$ is real distance between mobile *i* and BS $\tilde{j}$ and $n_{i\tilde{j}} \sim N(0,\sigma_{i\tilde{j}}^2)$ is modeled as additive white Gaussian noise (AWGN). We further denote *A* as a distance function as follow

$$A_{i\tilde{j}}(\theta_i) = \left\| \theta_i - BS_{\tilde{j}} \right\|, \tilde{j} = 1,2,...N \qquad (2.2)$$

where $\theta_i = \begin{bmatrix} x_i & y_i & z_i \end{bmatrix}^T$ is the unknown coordinate vector of mobile *i* and $BS_{\tilde{j}} = \begin{bmatrix} x_{\tilde{j}} & y_{\tilde{j}} & z_{\tilde{j}} \end{bmatrix}^T$ is the coordinate vector of BS $\tilde{j}$. From Figure 2.1, we focus on the position of mobile *i*, we can rewrite (2.1) in vector term by *N* measurement data as follow

$$d_i = A_i(\theta_i) + n_i \qquad (2.3)$$

where $d_i = \begin{bmatrix} d_{i\tilde{1}} \\ d_{i\tilde{2}} \\ \vdots \\ d_{i\tilde{N}} \end{bmatrix}, A_i(\theta_i) = \begin{bmatrix} A_{i\tilde{1}} \\ A_{i\tilde{2}} \\ \vdots \\ A_{i\tilde{N}} \end{bmatrix}, n_i = \begin{bmatrix} n_{i\tilde{1}} \\ n_{i\tilde{2}} \\ \vdots \\ n_{i\tilde{N}} \end{bmatrix}$ are the measurement vector, distance vector, and measurement error vector.

We want to utilize these measurements to estimate the position of mobile *i*. In Section 2.2, some typical LS estimators are introduced.

2.2 Least-Squares Algorithm

According to the model, the unknown position coordinate vector θ_i can be estimate based on least-squares theory by searching the minimum of the objective function,

$$\hat{\theta}_i = \min_{\theta_i} \left\{ \sum_{\tilde{j}=1}^{N} \frac{1}{\sigma_{i\tilde{j}}^2} \left(d_{i\tilde{j}} - \left\| \theta_i - BS_{\tilde{j}} \right\| \right)^2 \right\} \quad (2.4)$$

(2.4) is an optimal solution of LS estimator. It can be written as vector form as

$$\hat{\theta}_i = \arg\min_{\theta_i} \left\| d_i - A(\theta_i) \right\|_{W_i}^2 \quad (2.5)$$

where $\|\bullet\|_{W_i} = \sqrt{(\bullet)^T W_i (\bullet)}$ denotes a weighted norm with the weight matrix W_i which is chosen as the inverse of the measurement variance matrix, i.e., $W_i = \left(E\left[n_i n_i^T \right] \right)^{-1}$, where W_i is a diagonal matrix with $(\sigma_{i\tilde{j}}^2)^{-1}, \tilde{j} = 1 \sim N$ at *j*-th diagonal element. With the assumption of normally distributed of measurement errors, the Weighted Least-Squares estimator (WLS) [16] is identical to the Maximum Likelihood Estimator (MLE) [17]. In this thesis, weighting coefficient will be considered and revised in next chapter.

(2.5) is a nonlinear problem since *A* involves the norm term, it can be solved by iterative algorithm like the Steepest Descent method, the Newton method, the Gaussian-Newton (GN) method [8-9]. These methods provide equivalent solution when they

successfully converge. Our research bases on GN method. Section 2.1.1 introduces the GN method. In Section 2.2.2, some lineared LS methods are given. TLS framework which reduces the unknown parameter will be introduced in Section 2.2.3. TOA-based CRLB will be given in Section2.2.4.

2.2.1 Gauss-Newton Method

The basic idea of GN method is to linearize the signal model. From (2.2), the non-linear function $A_{i\tilde{j}}(\theta_i)$ can be linearized using Taylor series expansion

$$A_{i\tilde{j}}(\theta_i) = A_{i\tilde{j}}(\theta_{i,0}) + J_{i\tilde{j}}\left(\theta_i - \theta_{i,0}\right) + n_{ts,i\tilde{j}}, \tilde{j} = 1,2,...N \qquad (2.6)$$

where $n_{ts,i\tilde{j}}$ is the higher order truncation error of Taylor expansion, and the gradient vector $J_{i\tilde{j}} = \frac{(\theta_{i,0} - BS_{\tilde{j}})^T}{\left\|\theta_{i,0} - BS_{\tilde{j}}\right\|} = \left[\frac{x_{i,0} - x_{\tilde{j}}}{A_{i,\tilde{j}}} \quad \frac{y_{i,0} - y_{\tilde{j}}}{A_{i,\tilde{j}}} \quad \frac{z_{i,0} - z_{\tilde{j}}}{A_{i,\tilde{j}}}\right], \tilde{j} = 1,2,...N$. Then (2.3) becomes

$$d_i = A_i(\theta_{i,0}) + J_i(\theta_i - \theta_{i,0}) + n_{uncoop,i} \qquad (2.7)$$

where $\theta_{i,0}$ is the initial vector and $n_{uncoop,i} = n_{ts,i} + n_i$ denotes the total error including higher order truncation error of Taylor expansion and measurement noise, where $n_{ts,i} = \begin{bmatrix} n_{ts,i\tilde{1}} \\ n_{ts,i\tilde{2}} \\ \vdots \\ n_{ts,i\tilde{N}} \end{bmatrix}^T$. $J_i \in R^{N\times 3}$ (3 dimensions) is uncooperative Jacobian matrix [18],

$$J_i = \begin{bmatrix} J_{i\tilde{1}} \\ J_{i\tilde{2}} \\ \vdots \\ J_{i\tilde{N}} \end{bmatrix} = \begin{bmatrix} \frac{x_{i,0} - x_{\tilde{1}}}{A_{i\tilde{1}}} & \frac{y_{i,0} - y_{\tilde{1}}}{A_{i\tilde{1}}} & \frac{z_{i,0} - z_{\tilde{1}}}{A_{i\tilde{1}}} \\ \frac{x_{i,0} - x_{\tilde{2}}}{A_{i\tilde{2}}} & \frac{y_{i,0} - y_{\tilde{2}}}{A_{i\tilde{2}}} & \frac{z_{i,0} - z_{\tilde{2}}}{A_{i\tilde{2}}} \\ \vdots & \vdots & \vdots \\ \frac{x_{i,0} - x_{\tilde{N}}}{A_{i\tilde{N}}} & \frac{y_{i,0} - y_{\tilde{N}}}{A_{i\tilde{N}}} & \frac{z_{i,0} - z_{\tilde{N}}}{A_{i\tilde{N}}} \end{bmatrix} \qquad (2.8)$$

According to (2.7), the estimate location of the mobile *i* (2.5) can be written as

$$\hat{\theta}_i = \arg\min_{\theta_i} \left\| d_i - A_i(\theta_{i,0}) - J_i(\theta_i - \theta_{i,0}) \right\|^2_{W_{uncoop}} \qquad (2.9)$$

the GN method solves the problem by iteratively minimizing the new objective function,

$$\hat{\theta}_{i,k+1} = \hat{\theta}_{i,k} + (J_{i,k}{}^T W_{uncoop,i,k} J_{i,k})^{-1} J_{i,k}{}^T W_{uncoop,i,k} (d_i - A_i(\hat{\theta}_{i,k})) \qquad (2.10)$$

where the weighting matrix is covariance inverse of $n_{uncoop,i}$,

$$W_{uncoop,i,k} = \left(E\left[n_{uncoop,i,k} n^T_{uncoop,i,k} \right] \right)^{-1} \qquad (2.11)$$

The element of $W_{uncoop,i,k}$ is a diagonal matrix with

$$E\left[n_{uncoop,i,k} n^T_{uncoop,i,k} \right]_{\tilde{j}\tilde{j}} = \sigma^2_{ts,i\tilde{j},k} + \sigma^2_{i\tilde{j}}, \tilde{j} = 1 \sim N \qquad (2.12)$$

In (2.10), there exists 3×3 matrix inverse with highly computational cost. Note that we can omit the Taylor truncation error if there is a good reference point. In (2.10), $J_{i,k}$, $A_i(\theta_{i,k})$ can affect the position accuracy and will be updated with the *k*-th $\theta_{i,k}$. The GN method explores the quadratic form of the objective function and is adequate for solving (small-residual) non-linear problem, but the complexity is cumbersome. In next Section, three linearization algorithms will be introduced to reduce its computational cost.

2.2.2 Linearization of Least-Squares Method

There are three common linearization methods, Taylor-series expansion algorithm (TS) [10], distance-augmented algorithm (DA) [11] and hyperbolic-canceled algorithm [12]. We summarize them as follows. By linearizing the non-linear term, (2.2) can be written as

$$b = H\theta_i + n_L \qquad (2.13)$$

the terms b, H of three linearization methods had been derived in the literature. Applying weighted least-squares to get the closed form solution

$$\hat{\theta}_i = (H^T W_L H)^{-1} H^T W_L b \qquad (2.14)$$

where W_L is the weighted matrix. The covariance matrix of $e_i = \hat{\theta}_i - \theta_i$ is

$$\text{cov}(e_i) = \left(H^T W_L H \right)^{-1} \qquad (2.15)$$

and the Mean-Square-Error (MSE) of the estimator is

$$MSE = trace(\text{cov}(e_i)) \qquad (2.16)$$

The LLS estimators are easy to operate and cost less computation compared with iterative methods. It is trade-off between cost and accuracy. Some researches try to reduce the complexity with high accuracy. [19] utilize constrained least-squares method. [20] uses one range measurement in each iteration to update the user position. We introduce transformed least-squares (TLS) framework [13] which reduced the parameter of unknown parameters in Section 2.2.3.

2.2.3 Transformed Least-Squares Framework

Instead of the traditional LS estimator, Transformed Least-Squares (TLS) [13] tries to keep the required computations low in two steps. The first step is transforming the positioning problem to lower dimensions. There are three dimensions (3-D) in original 3-D localization problem. Once the dimensions are less, the unknown parameters to be estimated are less respectively. Second, solve the remaining parameters iteratively. [13] proposed a one dimensional iterative (1DI) method that the LLS method is used to transform the problem to one dimension and an iterative method is used to estimate the 1-D unknown parameter.

Actually, the idea of TLS can be explained as follow. In classical nonlinear LS (NLS) algorithm (2.4), the unknowns are estimated together. On the other hand, it can be divided to one unknown (z_i) nonlinear problem and other two dimension (x_i, y_i) nonlinear estimation. Assume that z_i parameters are fixed, x_i and y_i can be transformed to linear function of

z_i, the estimation problem become one dimension, i.e.,

$$\hat{\theta}_i = \min_{x_i, y_i, z_i} f(x_i, y_i, z_i) = \min_{z_i} \min_{x_i, y_i} f(x_i, y_i, z_i) \approx \min_{z_i} f(x_i(z_i), y_i(z_i), z_i) \quad (2.17)$$

f denotes objective function in (2.4). From (2.17), [13] divides the original three dimensions nonlinear problem to one dimension since the x-axis and y-axis coordinate of mobile *i* is transferred to linear function of z_i. The reduced-dimension localization problem can be solved based on the GN method introduced in Section 2.2.1. In [13], the mapping function is given based on hyperbolic-canceled algorithm mentioned in Section 2.2.2,

$$\left[\hat{x}_i \ \hat{y}_i\right]^T = m(b - H_2 z_i) \quad (2.18)$$

where $b_{\tilde{j}} = d_{\tilde{j}}^2 - d_{\tilde{N}}^2 - BS_{\tilde{i}}^T BS_{\tilde{i}} + BS_{\tilde{N}}^T BS_{\tilde{N}}$, $\tilde{j} = 1 \sim N$,

$$m = (H_1 W_L H_1)^{-1} H_1 W_L$$

$$H = \begin{bmatrix} H_1 & H_2 \end{bmatrix} = -2 \begin{bmatrix} \underbrace{\begin{matrix} x_{\tilde{1}} - x_{\tilde{N}} & y_{\tilde{1}} - y_{\tilde{N}} \\ \vdots & \vdots \\ x_{\tilde{N}-\tilde{1}} - x_{\tilde{N}} & y_{\tilde{N}-\tilde{1}} - y_{\tilde{N}} \end{matrix}}_{H_1} & \underbrace{\begin{matrix} z_{\tilde{1}} - x_{\tilde{N}} \\ \vdots \\ z_{\tilde{N}-\tilde{1}} - z_{\tilde{N}} \end{matrix}}_{H_2} \end{bmatrix}.$$

The mapping in (2.18) is fixed by mapping coefficients H_1, H_2 and *b*. Based on (2.18), the position of mobile *i* can be written as

$$\theta_i = \begin{bmatrix} x_i & y_i & z_i \end{bmatrix}^T = f + F z_i \quad (2.19)$$

where $f = \begin{bmatrix} mb \\ 0 \end{bmatrix}$, $F = \begin{bmatrix} -mH_2 \\ 1 \end{bmatrix}$, $f, F \in R^3$. Then, (2.5) can be written as

$$\hat{z}_i = \arg\min_{z_i} \left\| d_i - A(f + F z_i) \right\|_{W_i}^2 \quad (2.20)$$

Finally, the problem has transformed to one dimension nonlinear Least-Square problem according to the variable z_i, which can be solved by GN method iteratively. The TLS method not only reduces the computations but preserves performance comparable with GN method. In cooperative localization, the dimensions of unknowns are quite high by the positions of

mobiles. We propose a dimension reduced Least-Squares algorithms based on TLS framework, and the additional challenge from measurements between mobiles are another issue which will be described in Chapter 3.

2.2.4 Cramer-Rao Lower Bound

In previous section, mobile *i* can be estimated through uncooperative measurements. For comparison with these estimators, the CRLB is given as a criterion. Based on [22], the error covariance matrix of position error vector $\hat{e}_i = \hat{\theta}_i - \theta_i$ satisfies Information Inequality

$$\mathrm{cov}(\hat{e}_i) = E\left[\hat{e}_i \hat{e}_i^T\right] \geq I_{\theta_i}^{-1} \qquad (2.21)$$

where $I_{\theta_i}^{-1}$ is the full uncooperative Fisher Information Matrix (FIM) for mobile *i*

$$I_{\theta_i} = \sum_{\tilde{j}=1}^{N} \frac{1}{\sigma_{i\tilde{j}}^2} \begin{bmatrix} \frac{(x_i - x_{\tilde{j}})^2}{A_{i\tilde{j}}^2} & \frac{(x_i - x_{\tilde{j}})(y_i - y_{\tilde{j}})}{A_{i\tilde{j}}^2} & \frac{(x_i - x_{\tilde{j}})(z_i - z_{\tilde{j}})}{A_{i\tilde{j}}^2} \\ \frac{(x_i - x_{\tilde{j}})(y_i - y_{\tilde{j}})}{A_{i\tilde{j}}^2} & \frac{(y_i - y_{\tilde{j}})^2}{A_{i\tilde{j}}^2} & \frac{(y_i - y_{\tilde{j}})(z_i - z_{\tilde{j}})}{A_{i\tilde{j}}^2} \\ \frac{(x_i - x_{\tilde{j}})(z_i - z_{\tilde{j}})}{A_{i\tilde{j}}^2} & \frac{(y_i - y_{\tilde{j}})(z_i - z_{\tilde{j}})}{A_{i\tilde{j}}^2} & \frac{(z_i - z_{\tilde{j}})^2}{A_{i\tilde{j}}^2} \end{bmatrix} \qquad (2.22)$$

Then, the trace of inverse of $I_{\theta_i}^{-1}$ in (2.21) is defined as the lower bound for MSE, Therefore, uncooperative CRLB is given by

$$CRLB_{uncoop} = tr\left[I_{\theta_i}^{-1}\right] \qquad (2.23)$$

In cooperative system, the cooperative CRLB will be introduced in Section 3.1.3.

Chapter 3
Cooperative Localization System

Cooperative localization is raising up as a new branch of wireless localization in which several researches are being explored. By the development of short-range communication such as UWB, the direct communication of different terminals can be used in cooperative positioning. [17] considers that the short-range measurements are reliable to enhance the accuracy of location and investigate the data fusion of large-scale and small-scale.

In cooperative system, the distance measurements between any pairs of unknown positions mobiles are utilized to improve the location estimation. To mobile *i*, the measurement distances between BSs and the other mobiles are combined as the information of which are used to solve the estimation problem. The other unknown mobiles play a role as virtual BSs to assist mobile *i* in localization. In cooperative localization, the location accuracy of virtual BS is important since the un-precise virtual BS may cause the degradation of localization. It is a more critical task than conventional localization due to the additional information from mobiles to mobiles. Figure 3.1 indicates the cooperative localization system. There are *N* known positions of BSs and *M* unknown positions of mobiles. Our purpose is to estimate all the *M* unknown positions of mobiles by using total $(M \times N + C(M, 2))$ measurement data. From figure 3.1, mobile *i* receives *N* TOA measurement from known positions of BS and (*M*-1) measurements from unknown positions of mobile. $A_{i\tilde{j}}$ is the real distance between mobile *i* and BS $\tilde{j}$ which is mentioned in section 2.1; the cooperative term A_{ij} is denoted as the real distance between mobile *i* and mobile *j*.

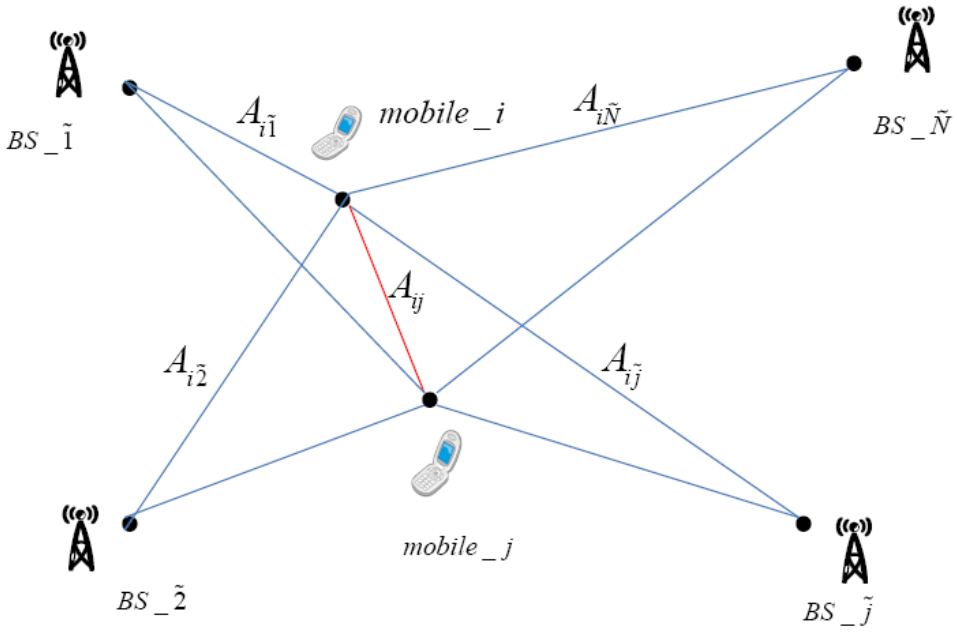

Figure 3.1 Cooperative localization system

The cooperative measurement between mobile *i* and mobile *j* is denoted as

$$d_{ij} = A_{ij} + n_{ij},\ i < j,\ i = 1,2,..,M-1,\ j = i, i+1,..,M \qquad (3.1)$$

where $n_{ij} \sim N(0, \sigma_{ij}^2)$ is cooperative measurement error modeled as AWGN. Combining (2.1) and (3.1), the cooperative measurement model can be writtene as

$$d = A(\theta) + \underline{n} \qquad (3.2)$$

where $\theta = \begin{bmatrix} \theta_1^T & \theta_2^T & \cdots & \theta_M^T \end{bmatrix}^T$ is the position vector of *M* mobile and

$$d = \begin{bmatrix} d_1 \\ \vdots \\ d_N \\ d_{12} \\ \vdots \\ d_{M-1,M} \end{bmatrix}^T, A(\theta) = \begin{bmatrix} A_1 \\ \vdots \\ A_N \\ A_{12} \\ \vdots \\ A_{M-1,M} \end{bmatrix}^T, \underline{n} = \begin{bmatrix} n_1 \\ \vdots \\ n_N \\ n_{12} \\ \vdots \\ n_{M-1,M} \end{bmatrix}^T ; d, A, \underline{n} \in R^{M \times N + C(M,2)}.$$

Further denote $C(M,2) = \frac{M!}{(M-2)!2!}$. The *M* unknown position coordinates can be estimated by minimizing the cost function based on least-squares estimator and it is written as

$$\hat{\theta} = \min_{\theta} \left\{ \underbrace{\sum_{i=1}^{M} \sum_{\tilde{j}=1}^{N} \frac{1}{\sigma_{i\tilde{j}}^2} \left(d_{i\tilde{j}} - \left\| \theta_i - BS_{\tilde{j}} \right\| \right)^2}_{Noncooperation} + \underbrace{\sum_{\substack{i=1 \\ j>i}}^{M} \frac{1}{\sigma_{ij}^2} \left(d_{ij} - \left\| \theta_i - \theta_j \right\| \right)^2}_{cooperation} \right\} \quad (3.3).$$

$$= \arg\min_{\theta} \left\| d - A(\theta) \right\|_W^2$$

Compared with (2.4), (3.3) takes additional information in account and we can see that cooperative localization is a tough issue than uncooperative localization. On the other hand, the reliability of additional cooperative measurements is another issue; if the unreliable measurements are used (σ_{ij}^2 is large), the localization accuracy becomes worse. Simulation shows the influence on noise variance in Section 4.2.1.

There are several ways that can be used to solve LS estimator (3.3). Nonlinear iterative algorithms estimate the location with high performance, but the complexity is quite high. By linearized algorithm, the costs can be reduced, but the performance is sacrificed. Here, we propose three pre-linear methods with low complexity but good accuracy. The structure of the rest of this section is as follows. Section 3.1 discusses cooperative GN method. The pre-linear method of auxiliary mobiles is proposed in Section 3.2. Section 3.3 derives the dimension-reduced GN algorithm for target mobile. Weighting compensation and mobile selection are discussed in Section 3.4 and Section 3.5 respectively. In the end, the computation is compared in Section3.6.

3.1 Cooperative Gauss-Newton Method

In cooperative localization, GN method is also useful to solve (3.3). According to Section 2.2.1, the additional cooperative term is discussed. Section 3.1.1 derives joint GN method. Divided GN method is given in Section3.1.2.

3.1.1 Joint GN Method

We know that unknown positions of mobiles are involved in cooperative system. In addition to (2.1), the remaining task is to linearize cooperative nonlinear distance function

$$A_{ij}(\theta_i, \theta_j) = \left\| \theta_i - \theta_j \right\| \qquad (3.4)$$

Apply Taylor-series expansion to (3.4) with initial value $\theta_{i,0}, \theta_{j,0}$ as follows

$$A_{ij}(\theta_i, \theta_j) = A_{ij}(\theta_{i,0}, \theta_{j,0}) + \left[\frac{\partial^T}{\partial_{\theta_i, \theta_j}} A_{ij}(\theta_{i,0}, \theta_{j,0}) \right] \Delta + n_{ts,ij}$$

where $n_{ts,ij}$ is the higher order truncation error of the Taylor-series expansion for A_{ij},

$$\frac{\partial^T}{\partial_{\theta_i, \theta_j}} A_{ij}(\theta_{i,0}, \theta_{j,0}) = \left[\frac{\partial A_{ij}(\theta_{i,0}, \theta_{j,0})}{\partial_{\theta_i}} \quad \frac{\partial A_{ij}(\theta_{i,0}, \theta_{j,0})}{\partial_{\theta_j}} \right] = \left[h_{ij}^T \quad -h_{ij}^T \right],$$

and h_{ij} is the cooperative gradient vector between mobile *i* and mobile *j*.

$$h_{ij} = \frac{\left(\theta_{i,0} - \theta_{j,0} \right)}{\left\| \theta_{i,0} - \theta_{j,0} \right\|}, \Delta = \begin{bmatrix} \theta_i - \theta_{i,0} \\ \theta_j - \theta_{j,0} \end{bmatrix} \qquad (3.5)$$

Now the cooperative measurement model (3.1) becomes

$$d_{ij} = A_{ij}(\theta_{i,0}, \theta_{j,0}) + \left[h_{ij}^T \quad -h_{ij}^T \right] \Delta + n_{coop,ij} \qquad (3.6)$$

where $n_{coop,ij} = n_{ts,ij} + n_{ij}$ denotes total cooperative error including Taylor truncation error and cooperative measurement error. (3.6) is a linear equation of cooperative measurement model. Collecting all the uncooperative linear equation (2.6) and cooperative linear equation (3.6) with *M*=4, joint GN Jacobian matrix equation is given by

$$d = A(\theta_0) + J(\theta - \theta_0) + n \qquad (3.7)$$

where $J = \begin{bmatrix} J_1 & 0 & 0 & 0 \\ 0 & J_2 & 0 & 0 \\ 0 & 0 & J_3 & 0 \\ 0 & 0 & 0 & J_4 \\ h_{12}^T & -h_{12}^T & 0 & 0 \\ h_{13}^T & 0 & -h_{13}^T & 0 \\ h_{14}^T & 0 & 0 & -h_{14}^T \\ 0 & h_{23}^T & -h_{23}^T & 0 \\ 0 & h_{24}^T & 0 & -h_{24}^T \\ 0 & 0 & h_{34}^T & -h_{34}^T \end{bmatrix}$, $n = \begin{bmatrix} n_{uncoop} \\ n_{coop} \end{bmatrix} = \begin{bmatrix} n_1 + n_{ts,1} \\ n_2 + n_{ts,2} \\ n_3 + n_{ts,3} \\ n_4 + n_{ts,4} \\ n_{12} + n_{ts,12} \\ n_{13} + n_{ts,13} \\ n_{14} + n_{ts,14} \\ n_{23} + n_{ts,23} \\ n_{24} + n_{ts,24} \\ n_{34} + n_{ts,34} \end{bmatrix}$ (3.8)

J is cooperative Jacobian matrix. The term uncooperative Jacobian matrix J_i is same as (2.8), $d, A(\theta_0), \in R^{M\times N+C(M,2)}$ are the measurement data, distance function which contained both uncooperative and cooperative term. Further denotes n is the total error vector including Taylor high order truncation error and noise. According to (3.7), the objective function is denoted as

$$\hat{\theta} = \arg\min_{\theta} \left\| d - A(\theta_0) - J(\theta - \theta_0) \right\|_W^2 \qquad (3.9)$$

and the joint GN estimator solves (3.9) iteratively by

$$\hat{\theta}_{k+1} = \hat{\theta}_k + (J_k{}^T W_k J_k)^{-1} J_k{}^T W_k (d - A(\hat{\theta}_k)) \qquad (3.10)$$

$$W_k = (E\left[n_k n_k{}^T \right])^{-1} = \begin{bmatrix} W_{uncoop,k} & 0 \\ 0 & W_{coop,k} \end{bmatrix}$$

Here, J_k denotes *kth* cooperative Jacobian matrix which is different from J_i in (2.8). and $W_{coop,k}$ is covariance inverse of $n_{coop,k}$,

$$W_{coop,k} = \left(E\left[n_{coop,k} n_{coop,k}^T \right] \right)^{-1}$$

The element of $E\left[n_{coop,k} n_{coop,k}^T \right]$ is a diagonal matrix with

$$E\left[n_{coop,k}n_{coop,k}^{T}\right]=\begin{bmatrix}\sigma_{ts,12,k}^{2}+\sigma_{12}^{2} & & 0\\ & \ddots & \\ 0 & & \sigma_{ts,12,k}^{2}+\sigma_{(M-1)M}^{2}\end{bmatrix}$$

W_k is a diagonal matrix which including $W_{uncoop,k}$ in (2.12) and cooperative term. Note that there is $3M\times 3M$ inverse matrix $(J_k{}^{T}W_kJ_k)^{-1}$ in (3.10) which includes highly computational cost. Besides, we can omit the Taylor truncation error as before if there is a good reference point. In Section 4.4.1, the effect on Taylor truncation error from initial value will be shown. In (3.10), the positions of mobiles are updated jointly with high position accuracy. In section 3.1.2, the divided method which updates the position of mobile individually will be described.

3.1.2 Divided GN Method

We know that if there exists a mobile *j* with known position, it can be regarded as a virtual BS to mobile *i* and can be helpful to estimate mobile *i*. Figure 3.2 illustrates the above description.

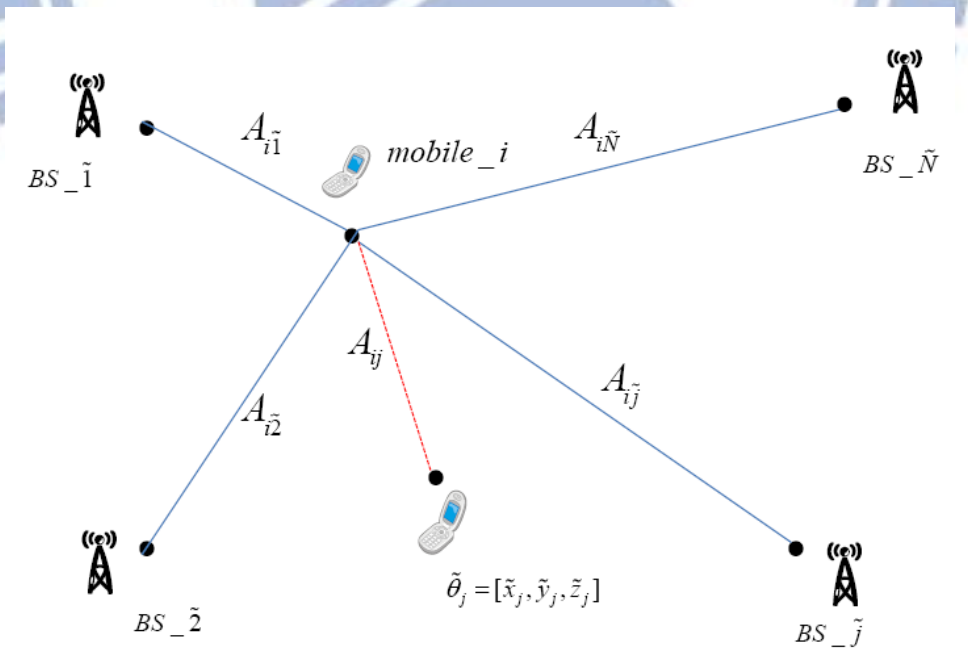

Figure 3.2 Cooperative localization with virtual BS $\tilde{\theta}_j$

From Figure 3.2, the position of every single mobile can be estimated by measurements from true BSs and other virtual BSs. To mobile *i*, the LS searches a $\hat{\theta}_i$ which minimizes the objective function

$$\hat{\theta}_i = \min_{\theta_i} \left\{ \underbrace{\sum_{\tilde{j}=1}^{N} \frac{1}{\sigma_{i\tilde{j}}^2} \left(d_i - \left\| \theta_i - BS_{\tilde{j}} \right\| \right)^2}_{noncooperation} + \underbrace{\sum_{j=1, j\neq i}^{M} \frac{1}{\sigma_{ij}^2} \left(d_{ij} - \left\| \theta_i - \tilde{\theta}_j \right\| \right)^2}_{cooperation} \right\}, i = 1, 2, .., M \qquad (3.11)$$

where $\tilde{\theta}_j$ denotes known position of virtual BS. Note that (3.11) only include the unknown parameter of mobile *i*. However, the uncertain positions of virtual BSs may degrade the accuracy. To deal with this problem, the individual uncooperative localization (2.4) is used to find a not-bad initial value of virtual BS. Then, (3.11) estimates the positions of mobile *i*.

$$\hat{\theta}_i = (H_i^T W_{L,i} H_i)^{-1} H_i^T W_{L,i} b_i \qquad (3.12)$$

Every individual mobile can be updated by other *M-1* virtual BSs iteratively to improve the position accuracy. Actually, Jacobi and Gauss-Seidel methods [18] are used to choose the positions of virtual BSs. Our proposed parallel and sequential pre-linear methods are based on Jacobi and Gauss-Seidel methods, respectively. Figure 4.6 shows the comparison between divided method and pre-linear methods. The divided method can reduce the computation costs most in (3.10), but the performance is sacrificed.

3.1.3 Cooperative CRLB

In cooperative system, cooperative CRLB is given as uncooperative system that is to be a standard to estimators in this Chapter. The full cooperative Fisher Information Matrix can be written as follows

$$I_\theta = \begin{bmatrix} I_{\theta_1} + \sum_{\substack{i=1 \\ i\neq 1}}^{M} \mathbf{C}_{1i} & -\mathbf{C}_{12} & \vdots & -\mathbf{C}_{1M} \\ -\mathbf{C}_{12} & I_{\theta_2} + \sum_{\substack{i=1 \\ i\neq 2}}^{M} \mathbf{C}_{2i} & \cdots & -\mathbf{C}_{2M} \\ \vdots & \vdots & \ddots & \vdots \\ -\mathbf{C}_{1M} & -\mathbf{C}_{2M} & \cdots & I_{\theta_M} + \sum_{\substack{i=1 \\ i\neq M}}^{M} \mathbf{C}_{Mi} \end{bmatrix} \qquad (3.13)$$

where I_{θ_i} is the uncooperative FIM in (2.21) for mobile *i* and $\mathbf{C}_{ij}$ is cooperative information matrix between mobile *i* and mobile *j* which is denoted as

$$\mathbf{C}_{ij} = \frac{1}{\sigma_{ij}^2} \begin{bmatrix} \frac{(x_i - x_j)^2}{A_{ij}^2} & \frac{(x_i - x_j)(y_i - y_j)}{A_{ij}^2} & \frac{(x_i - x_j)(z_i - z_j)}{A_{ij}^2} \\ \frac{(x_i - x_j)(y_i - y_j)}{A_{ij}^2} & \frac{(y_i - y_j)^2}{A_{ij}^2} & \frac{(y_i - y_j)(z_i - z_j)}{A_{ij}^2} \\ \frac{(x_i - x_j)(z_i - z_j)}{A_{ij}^2} & \frac{(y_i - y_j)(z_i - z_j)}{A_{ij}^2} & \frac{(z_i - z_j)^2}{A_{ij}^2} \end{bmatrix} \qquad (3.14)$$

Then, the cooperative CRLB for mobile *i* is

$$CRLB_{coop} = tr\left[I_\theta^{-1} \right] \qquad (3.15)$$

Note that the cooperative CRLB for mobile *1* lies at the upper-left block

$$CRLB_{coop,mobile_1} = tr\left[\text{upper-left } 3\times 3 \text{submatrix of } I_\theta^{-1} \right]$$

Simulation compares our methods with (3.15) in Section 4.1. In Section 3.2, we propose a low complexity with high accuracy pre-linear methods in cooperative localization.

3.2 Pre-Linear Methods of Auxiliary Mobiles

In cooperative system, the *M* mobiles positioning problem is presented. In Section 3.1, joint GN method outperforms divided method, but the total costs are higher than divided method. Instead of GN method, we try to seek a relation between mobiles by re-formulating the positioning problem to reduce the number of unknown mobiles based on [13]. In this way, we expect that the proposed pre-linear methods have good performance in both accuracy and

complexity. The basic idea of pre-linear method consists of two steps: The unknown of parameters are reduced in step 1 by pre-linear mapping, and the localization algorithm for remaining unknown parameters in step 2 using the pre-linear function in step 1. Figure 3.3 indicates the flowchart of the pre-linear method. In Figure 3.3, we aim at searching a mapping function between unknown positions of mobiles.

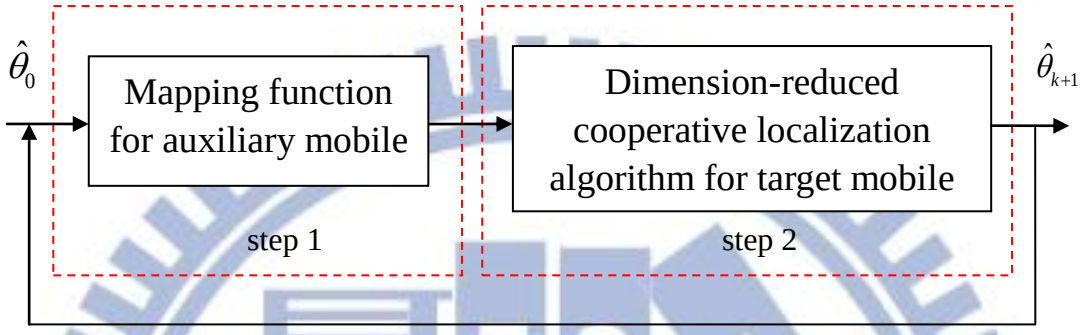

Figure 3.3 Flowchart of pre-linear method

In cooperative localization, mobiles exchange the information collaboratively, so we focus on the mapping between mobile-to-mobile. Unlike [13], the cooperative measurement between mobile *i* and mobile *j* $\|\theta_i - \theta_j\|$ cannot be linearized by squaring the distance function (3.4) since both θ_i and θ_j are unknown parameters. Fortunately, the Taylor-Series expansion can linearize the equation which describes in Section 3.1.1. Furthermore, the pre-linear method works iteratively while pre-linear mapping in [13] is fixed. On the other hand, the actual mapping relations between mobiles are not existence, we can also correct the mapping by iteration.

Once the pre-linear mapping is obtained, the dimension of unknown parameters to be estimated can be reduced, and the localization algorithm is simplified accordingly. However, there is a lot of combination of mapping relation, the choice of mapping function is based on different localization requirement. Our purpose is to simplify the algorithm in (3.10), so the linear mapping is a suitable choice which reduces the complexity most. The following

describes the two steps of the pre-linear method.

In Step 1, we select a mobile called "Target" mobile which is chosen as a reference mobile to be estimated in step 2; and the others called "Auxiliary" mobiles that are restricted to be a linear function of the target mobile. It is assumed that there exists some linear mapping relation between auxiliary mobile and target mobile. Without loss of generality, we select mobile *1* as a target mobile, and mobile *2* ~*M* as auxiliary mobiles, i.e., $\theta_q = L_q(\theta_1)$, q =*2,3,…,M*. Therefore, (3.2) can be rewritten as

$$d = A\left(\theta_1, L_1(\theta_1), L_2(\theta_1), .., L_M(\theta_1)\right) + n \qquad (3.16)$$

By linear mapping function *L*, the auxiliary mobiles can be transformed to the linear function of the target mobile. However, mobiles are located at different positions independently so an error-free mapping is usually not available. How to find a proper mapping function by measurement data becomes a critical issue. We propose three linearized mapping methods to implement the mapping function. The detail will be described in the next section.

In Step 2, once the mapping function is generated, LS estimator can solve the dimension-reduced cooperative localization problem based on (3.16).

$$\hat{\theta}_1 = \arg\min_{\theta_1} \left\| d - A(\theta_1, L_1(\theta_1), L_2(\theta_1), .., L_M(\theta_1)) \right\|_W^2 \qquad (3.17)$$

We only consider the parameters of target mobile in this step unlike the original multiple mobiles in (3.3). In section 3.3, Dimension-reduced GN method is derived based on the GN algorithm mentioned at section 3.1. The original $3M \times 3M$ (3-D case) inverse matrix problem in (3.10) can be transferred to 3×3 positioning problem. Therefore, the computation cost is reduced efficiently. The detail of computation costs will be described in Section 3.6.

We note that if the position of target mobile is updated, the corresponding positions of auxiliary mobiles can be obtained by using mapping function and the position of target mobile we estimated. Figure 3.4 indicates the description above.

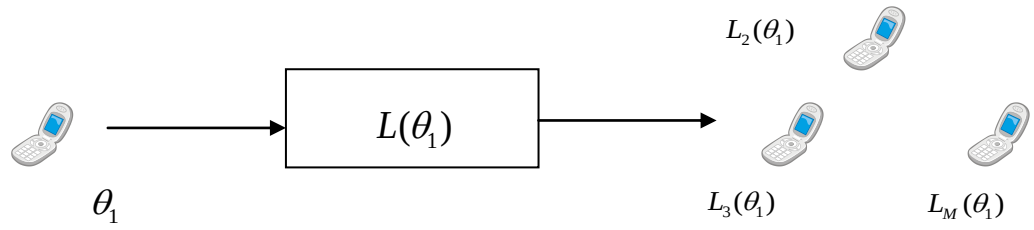

Figure 3.4 The diagram of mapping from target mobile to auxiliary mobiles

In Figure 3.4, the accuracy of target mobile affects the accuracy of auxiliary mobiles by the mapping function $L(\theta_1)$. The reliable target mobile can improve the accuracy of auxiliary mobiles. In Section 3.5, we propose a target mobile selection method to find the reliable target mobile. In fact, the auxiliary mobiles are used cooperatively to search the mapping function which is inserted in the cost function in step 2 (see (3.17)), so auxiliary mobiles and target mobile interact with each other. The uncertain position of mobiles may deteriorate the localization accuracy. Therefore, the compensation of weighting coefficient will be derived in Section 3.4.

3.2.1 Joint Pre-Linear Method

There are *M* unknown positions of mobile in localization system. Our purpose is to find the relation between these *M* positions of mobile which is described in previous section.

In joint pre-linear method, we want to find a mapping function so that all the (*M*-1) auxiliary mobiles can be written as a function of target mobile jointly. i.e.,

$$\begin{bmatrix} \theta_2^T & \theta_3^T & \cdots & \theta_M^T \end{bmatrix}^T = L(\theta_1) \qquad (3.18)$$

where *L* is a linear mapping from $R^3 \to R^{3(M-1)}$. Figure 3.5 depicts the mapping relation of joint pre-linear method.

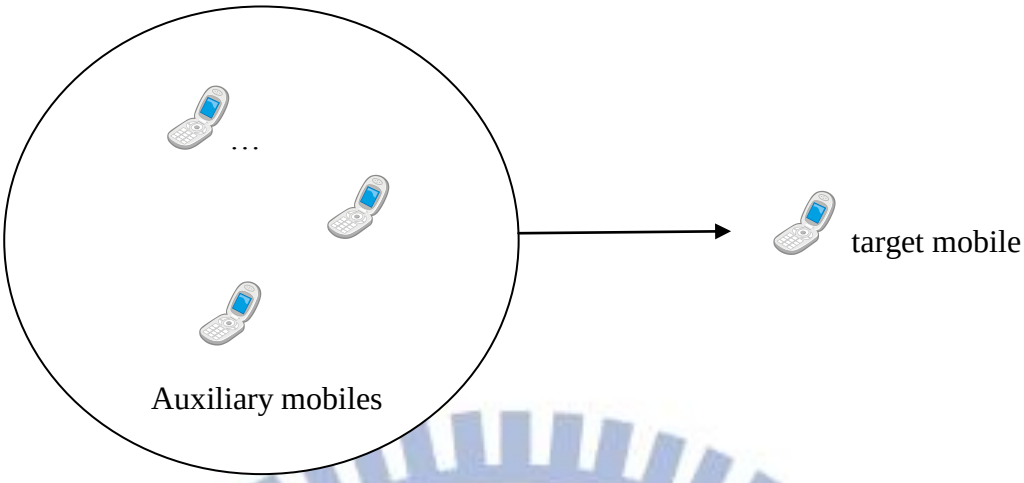

Figure 3.5 Mapping relation of joint pre-linear method

In Figure 3.5, all the auxiliary mobiles cooperate with each other jointly to find their relations with the target mobile. If (3.18) is known, the position vectors of auxiliary mobile are transformed to a function of the target mobile successfully and can help to locate the position of the target mobile. Mapping function plays an important role that it replaces the original positions of auxiliary mobile; in other words, the dimension has been reduced in step 2. The mapping function L will be derived in the next paragraph. The complete algorithm of joint pre-linear method is indicated in Figure 3.6.

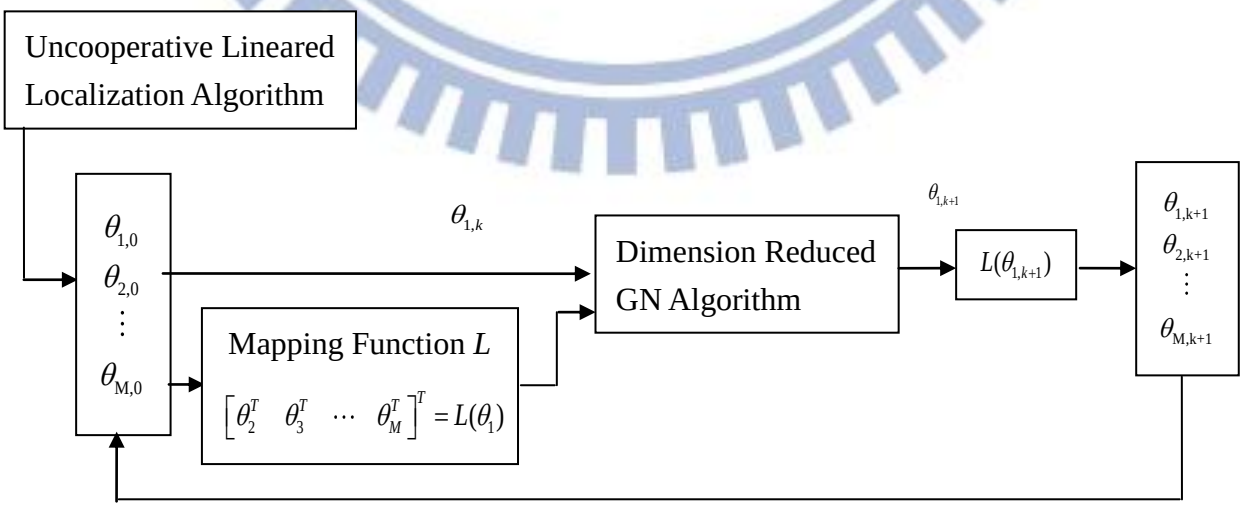

Figure 3.6 Joint pre-linear algorithm

Fortunately, we can get the mapping function by linearizing the cooperative nonlinear function (3.2) using Taylor-series expansion. Rearranging (3.7) with *M* mobiles and the linear equation is given

$$y = J\theta + n \qquad (3.19)$$

where *J* is cooperative Jacobian matrix which is same as (3.7),

$$y = \begin{bmatrix} y_{uncoop} \\ y_{coop} \end{bmatrix} = d + J\theta_0 ; y_{uncoop} \in R^{M \times N}, y_{coop} \in R^{C(M,2)}$$

We further denote F_i as the *i* column of *J*, and (3.19) can be rewritten as

$$y = \begin{bmatrix} F_1 & F_2 & \cdots & F_M \end{bmatrix} \begin{bmatrix} \theta_1 \\ \theta_2 \\ \vdots \\ \theta_M \end{bmatrix} + n \qquad (3.20)$$

Note that θ_1 is the position vector of the target mobile. From (3.20), we can see that if we regard θ_1 as a variable parameter of equation and shift the term $F_1\theta_1$ to the left-hand side of the equation as follows,

$$y - F_1\theta_1 = \begin{bmatrix} F_2 & F_3 & \cdots & F_M \end{bmatrix} \begin{bmatrix} \theta_2 \\ \theta_3 \\ \vdots \\ \theta_M \end{bmatrix} + n \qquad (3.21)$$

the position vector of target mobile θ_1 is used to solve the linear equation (3.21) with unknowns $\theta' = \begin{bmatrix} \theta_2 & \theta_3 & \cdots & \theta_M \end{bmatrix}^T$. Note that the dimension in (3.20) is *3M* but *3(M-1)* in (3.21). According to (3.21), in the *k-th* iteration, the linear LS estimator mentioned in Section 2.1.2 can solve the problem as follow

$$\theta_k^{'} = (F_k^{'T} W_k F_k^{'})^{-1} F_k^{'T} W_k (y_k - F_{1,k}\theta_{1,k}) \qquad (3.22)$$

We denote auxiliary Jacobian matrix $F_k^{'} = \begin{bmatrix} F_{2,k} & F_{3,k} & \cdots & F_{M,k} \end{bmatrix}$, taget Jacobian matrix $F_{1,k}$, and weighting matrix is same as (3.10). The linear mapping function is generated successfully in (3.22). The terms $F_k^{'}$, $F_{1,k}$, and y_k include information of unknown parameter which are updated by the (*k*-1)-*th* solution shown in figure 3.6, we can understand that the mapping function is updated iteratively. We should note that $\theta_k^{'}$ is not the *k-th* iteration solution of auxiliary mobile since (3.22) is the function of variable $\theta_{1,k}$. The solution will be updated after the algorithm in step 2. In addition, (3.22) can be simplified as

$$\theta_k^{'} = g_{joint,k} + G_{joint.k}\theta_{1k} \qquad (3.23)$$

where

$$g_{joint,k} = (F_k^{'T} W_k F_k^{'})^{-1} F_k^{'T} W_k y_k \in R^{3(M-1)}$$

$$G_{joint,k} = -(F_k^{'T} W_k F_k^{'})^{-1} F_k^{'T} W_k F_{1,k} \in R^{3(M-1)\times 3} \qquad (3.24)$$

The mapping coefficients g_{joint} and G_{joint} will be updated and become more accurate by iteration. We can obtain the linear mapping between every single auxiliary mobile and target mobile by separating (3.23),

$$\theta_k^{'} = g_{joint,i,k} + G_{joint,i,k}\theta_{1,k}; i = 2,3,..,M \qquad (3.25)$$

In (3.25), we can see that the position vector of auxiliary mobiles becomes a linear function of position vector of target mobile. The linear mapping equation is generated by revising linear LS formulation. Here, we give a example if number of mobiles is equal to 4. The cooperative linear model in case *M=4* can be written as

$$\begin{bmatrix} y_{1,k} \\ y_{2,k} \\ y_{3,k} \\ y_{4,k} \\ y_{12,k} \\ y_{13,k} \\ y_{14,k} \\ y_{23,k} \\ y_{24,k} \\ y_{34,k} \end{bmatrix} = \begin{bmatrix} J_{1,k} & 0 & 0 & 0 \\ 0 & J_{2,k} & 0 & 0 \\ 0 & 0 & J_{3,k} & 0 \\ 0 & 0 & 0 & J_{4,k} \\ h_{12,k}^T & -h_{12,k}^T & 0 & 0 \\ h_{13,k}^T & 0 & -h_{13,k}^T & 0 \\ h_{14,k}^T & 0 & 0 & -h_{14,k}^T \\ 0 & h_{23,k}^T & -h_{23,k}^T & 0 \\ 0 & h_{24,k}^T & 0 & -h_{24,k}^T \\ 0 & 0 & h_{34,k}^T & -h_{34,k}^T \end{bmatrix} \begin{bmatrix} \theta_{1,k} \\ \theta_{2,k} \\ \theta_{3,k} \\ \theta_{4,k} \end{bmatrix} + \begin{bmatrix} n_{ts,1,k} + n_1 \\ n_{ts,2,k} + n_2 \\ n_{ts,3,k} + n_3 \\ n_{ts,4,k} + n_4 \\ n_{ts,12,k} + n_{12} \\ n_{ts,13,k} + n_{13} \\ n_{ts,14,k} + n_{14} \\ n_{ts,23,k} + n_{23} \\ n_{ts,24,k} + n_{24} \\ n_{ts,34,k} + n_{34} \end{bmatrix} \quad (3.26)$$

where

$$\tilde{r}_{i,k} = A_i(\theta_{i,k}) - J_i(\theta_{i,k})\theta_{i,k}$$

$$\tilde{r}_{ij,k} = A_{i,j}(\theta_{i,k}, \theta_{j,k}) + h_{ij,k}\theta_{i,k} - h_{ij,k}\theta_{j,k}$$

$$y_{i,k} = d_i - \tilde{r}_{i,k}\tilde{r}_{i,k}$$

$$y_{ij,k} = d_{ij} - \tilde{r}_{ij,k} \quad (3.27)$$

Note that the Taylor higher order truncation error can be omitted if the reference point is good enough. Here, there are 4N pairs of measurements between mobiles to BSs and *C(M,2)=6* pairs of cooperative measurement between mobiles. Based on (3.22), the mapping function can be written as

$$\begin{bmatrix} \theta_{2,k} & \theta_{3,k} & \theta_{4,k} \end{bmatrix}^T = (F_k^{'T} W_k F_k^{'})^{-1} F_k^{'T} W_k (y_{l,k} - F_{1,k}\theta_{1,k}) \quad (3.28)$$

where $F_k^{'} = \begin{bmatrix} F_{2,k} & F_{3,k} & F_{4,k} \end{bmatrix}$. We can see that the row *1~N* are zeros in F_k, and the mapping function is similar to the divided method which regards $\theta_{1,k}$ as a virtual BS with known position to other *M-1* mobiles. On the contrary, $\theta_{1,k}$ in (3.28) is still a variable parameter that will be updated in the next step; $F_{1,k}\theta_{1,k}$ is the revised term which adjust the cooperative measurement between target mobile and other *3* auxiliary mobile by gradient vector between

target mobile and auxiliary mobile j h_{1j}, $j = 2 \sim 4$, and the first element $J_{1,k}$ in $F_{1,k}$ is useless since $J_{1,k}$ is the term that related to the uncooperative measurement between target mobile and BSs. The detail of mathematical expression for (3.28) will be given in Section 3.6. With the linear mapping function, the original model can be changed to one unknown mobile problem; it is same as the following two pre-linear method. In Section 3.3, the dimension-reduced GN algorithm will be derived.

3.2.2 Parallel Pre-Linear Method

We have derived the joint pre-linear method in the previous Section. In (3.22), there still remains $3(M-1)\times 3(M-1)$ matrix inversion even though it is better than $3M \times 3M$ matrix inversion in original GN algorithm. Based on section 3.1.2, we can further reduce the complexity of the mapping function.

Instead of joint method, we can derive the mapping function individually in parallel pre-linear method based on Jacobi method [18]. The following figure depicts the mapping relation of parallel pre-linear method.

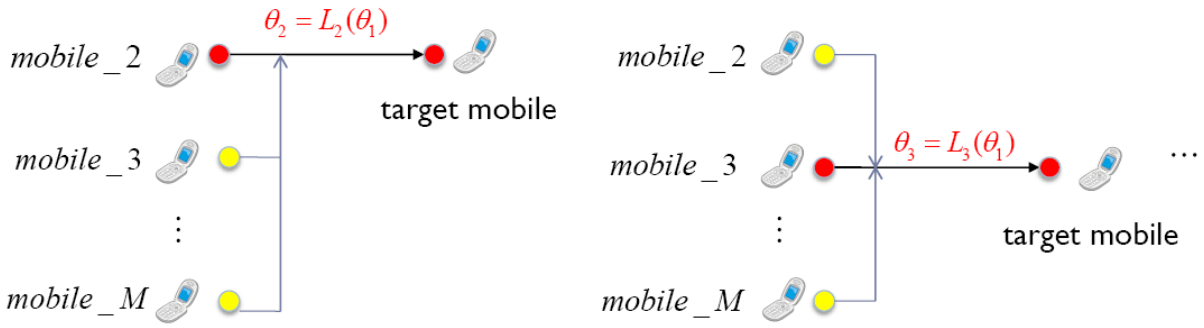

Figure 3.7 Mapping relation of parallel pre-linear method

We illustrate the parallel method for mobile 2 and mobile 3 in Figure 3.7. Auxiliary mobiles find the relation with target mobile individually. To auxiliary mobile q, it regards the

other (*M-2*) auxiliary mobile as virtual BSs; the localization scenario becomes *N* fixed BSs and (*M-2*) virtual BSs with two unknown positions of mobiles that contained one target and one auxiliary mobile. To every individual mobile in Jacobi method, other (*M-1*) are regarded as virtual BS with known position. In pre-linear methods, the position of target mobile is still unknown which is different from divided method, we find the linear mapping between auxiliary mobiles and target mobile and utilize the pre-linear function to estimate the position of target mobile. The LS estimator for mobile *1* (target mobile) and mobile *q* (auxiliary mobile) is given by

$$\begin{bmatrix}\hat{\theta}_1\\ \hat{\theta}_q\end{bmatrix}=\min_{\theta_1,\theta_q}\left\{\begin{bmatrix}\underbrace{\sum_{\tilde{j}=1}^{N}\frac{1}{\sigma_{1\tilde{j}}^2}\left(d_{1\tilde{j}}-\left\|\theta_1-BS_{\tilde{j}}\right\|\right)^2}_{Noncooperation}+\underbrace{\sum_{\substack{j=2\\ j\neq q}}^{M}\frac{1}{\sigma_{1j}^2}\left(d_{1j}-\left\|\theta_1-\tilde{\theta}_j\right\|\right)^2}_{\text{virtual BSs}}\\ \underbrace{+\sum_{\tilde{j}=1}^{N}\frac{1}{\sigma_{q\tilde{j}}^2}\left(d_{q\tilde{j}}-\left\|\theta_q-BS_{\tilde{j}}\right\|\right)^2}_{Noncooperation}+\underbrace{\sum_{\substack{j=2\\ j\neq q}}^{M}\frac{1}{\sigma_{qj}^2}\left(d_{qj}-\left\|\theta_q-\tilde{\theta}_j\right\|\right)^2}_{\text{virtual BSs}}\end{bmatrix}+\underbrace{\frac{1}{\sigma_{1q}^2}\left(d_{1q}-\left\|\theta_1-\theta_q\right\|\right)^2}_{cooperation}\right\};q=2\sim M \quad (3.29)$$

where $\tilde{\theta}_j$ denotes known position virtual BS. The complete algorithm of parallel pre-linear method is indicated in figure 3.8.

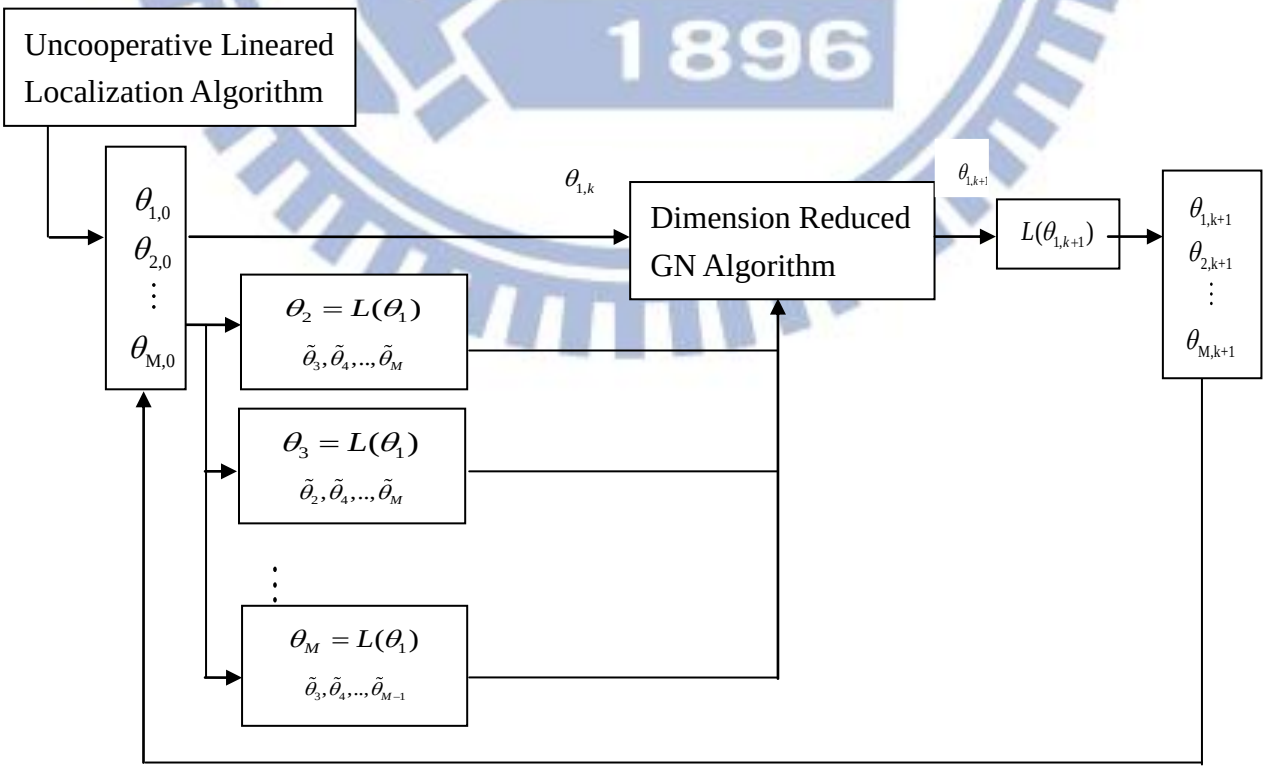

Figure 3.8 Parallel pre-linear algorithm

First, the position of virtual BSs are estimated by the uncooperative localization algorithm, and utilized to estimate the position of mobile. In each iteration, the mapping function can be generated in the sub-block of step 1 with the cooperation of virtual BSs. Then, the GN algorithm solves the position of target mobile using these mapping function as well as joint method. In the end, the target mobiles can be updated by the solution of GN algorithm and mapping function in step1. Note that the mapping function in each sub-block is obtained separately which is different from the joint method.

Based on (3.29), the linear TS equation in matrix form at *k*th iteration can be written as

$$y_{p\_q,k} = J_{p\_q,k}\theta_{p\_q,k} + n_{p\_q,k}, q = 2 \sim M \qquad (3.30)$$

where $\theta_{p\_q,k} = \begin{bmatrix} \theta_{1,k} & \theta_{q,k} \end{bmatrix}^T$. Without loss of generality, let *q=2*,

$$J_{p\_2,k} = \begin{bmatrix} J_{1,k} & 0 \\ h_{13,k}^T & 0 \\ \vdots & 0 \\ h_{1M,k}^T & 0 \\ 0 & J_{2,k} \\ 0 & h_{23,k}^T \\ 0 & \vdots \\ 0 & h_{2M,k}^T \\ h_{12,k}^T & -h_{12,k}^T \end{bmatrix} = \begin{bmatrix} J_{1,k} & 0 \\ v_{1,k} & 0 \\ 0 & J_{2,k} \\ 0 & v_{2,k} \\ h_{12,k}^T & -h_{12,k}^T \end{bmatrix} \qquad (3.31),$$

$J_{p\_2,k}$ denotes the cooperative Jacobian matrix for parallel method, where $v_{j,k} = \begin{bmatrix} h_{j3,k}^T & h_{j4,k}^T & \cdots & h_{jM,k}^T \end{bmatrix}^T ; j = 1,2$ denotes as virtual Jacobian matrix;

$$y_{p\_2,k} = \begin{bmatrix} y_{1,k} & y_{13,k} & \cdots & y_{1M,k} & y_{2,k} & y_{23,k} & \cdots & y_{2M,k} & y_{12,k} \end{bmatrix}^T \qquad (3.32),$$

and

$$n_{p\_2,k} = \begin{bmatrix} n_{uncoop,1,k} & n_{coop,13,k} & \cdots & n_{coop,1M,k} & n_{uncoop,2,k} & n_{coop,23,k} & \cdots & n_{coop,2M,k} & n_{coop,12,k} \end{bmatrix}^T$$

(3.33)

is the sum of Taylor truncation error and measurement noise. In (3.30), the *k-1* iteration solutions are used as the virtual BSs instead of the true position, so we further denote the location error at the *k*th iteration as follows

$$e_{j,k} = \tilde{\theta}_{j,k} - \theta_j, j = 1 \sim M \qquad (3.34)$$

The location error may degrade the location accuracy if the virtual BS is unreliable. In Section 3.4, the location error is considered and we will compensate its effect. The computer simulation shows the compensation in next chapter.

Denote $J_{p\_q,k} = \begin{bmatrix} F_{p\_q1,k} & F_{p\_q2,k} \end{bmatrix}$, based on (3.21), (3.30) can be written as

$$(y_{p\_q,k} - F_{p\_q1,k}\theta_{1,k}) = F_{p\_q2,k}\theta_{q,k} + n_{p\_q,k}; q = 2 \sim M \qquad (3.35)$$

The mapping function between $\theta_{q,k}$ and target mobile in Figure 3.8 is obtained as follows

$$\theta_{q,k} = g_{p\_q,k} + G_{p\_q,k}\theta_{1,k}; q = 2 \sim M$$

$$g_{p\_q,k} = \left(F_{p\_q2,k}^T W_{p\_q,k} F_{p\_q2,k}\right)^{-1} F_{p\_q2,k}^T W_{p\_q,k} y_{p\_q,k}$$

$$G_{p\_q,k} = -\left(F_{p\_q2,k}^T W_{p\_q,k} F_{p\_q2,k}\right)^{-1} F_{p\_q2,k}^T W_{p\_q,k} F_{p\_q1,k} \qquad (3.36).$$

where $W_{p\_q,k} = \left(E\left[n_{p\_q,k} n_{p\_q,k}^T\right]\right)^{-1}$ is a diagonal matrix with inverse of variance of noise and truncation error on the diagonal element. The mapping coefficients $g_{p\_q,k}$ and $G_{p\_q,k}$ are updated by iteration as joint method. The computation is reduced greatly in (3.36) since there is only 3×3 matrix inversion. The dimension-reduced GN algorithm solves the position of target mobile with these mapping function as well as joint method. In next Section, sequential pre-linear method, similar to parallel pre-linear method, will be given.

3.2.3 Sequential Pre-Linear Method

The difference between parallel pre-linear method and sequential pre-linear method is

that in the former, the information got at last iteration are parallelized used in the sub-block in the mapping function, i.e., $\left[\tilde{\theta}_{2,k-1} \quad \cdots \quad \tilde{\theta}_{i-1,k-1} \quad \tilde{\theta}_{i+1,k-1} \quad \cdots \quad \tilde{\theta}_{M,k-1}\right]$ are used as virtual BSs to mobile *i*; to mobile *j*, $\left[\tilde{\theta}_{2,k-1} \quad \cdots \quad \tilde{\theta}_{j-1,k-1} \quad \tilde{\theta}_{j+1,k-1} \quad \cdots \quad \tilde{\theta}_{M,k-1}\right]$ are utilized for mapping function searching. The idea of sequential pre-linear method comes from Gauss-Seidel method [18], the following figure depicts the mapping relation of sequential pre-linear method.

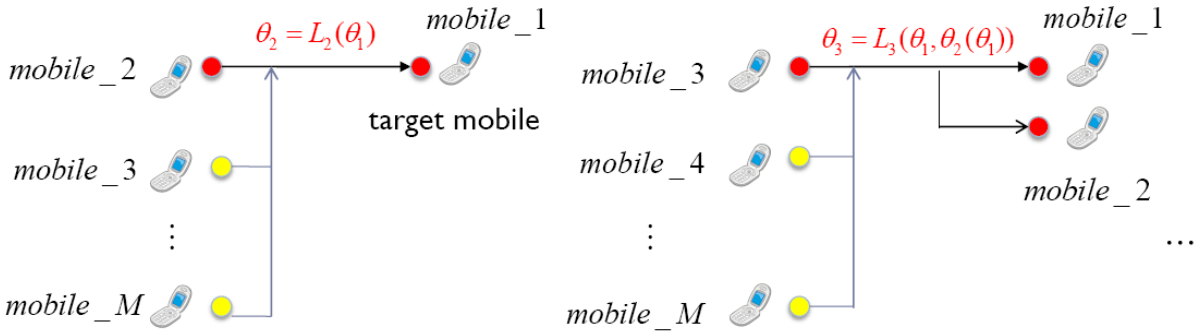

Figure 3.9 Mapping relation of sequential pre-linear method

From Figure 3.9, the pre-linear mapping is generated sequentially. To mobile 2, parallel and sequential are same. To mobile 3, mobile 4 ~M are regarded as virtual BSs and we want to find the linear relation between mobile 3 and target mobile (mobile 1) and mobile 2 (the virtual target). The pre-linear mapping function of mobile *2* can be used to find the mapping of mobile *3*, the mathematical expression is derived later. Then mapping of mobile *4* can be generated by cooperation with mapping of mobile *2* and mobile*3* respectively and so on. Sequential pre-linear method updates the mapping section by section in each iteration, and the mapping function is delivered among auxiliary mobiles. To mobile *q*, the LS estimator of sequential pre-linear method is given by

$$\hat{\theta}_{s,q}=\min_{\theta_{s,q}}\left\{\underbrace{\sum_{i=1}^{q}\sum_{\tilde{j}=1}^{N}\frac{1}{\sigma_{1\tilde{j}}^{2}}\left(d_{i\tilde{j}}-\left\|\theta_i-BS_{\tilde{j}}\right\|\right)^2}_{Noncooperation}+\underbrace{\sum_{i=1}^{q}\sum_{j=q+1}^{M}\frac{1}{\sigma_{ij}^{2}}\left(d_{ij}-\left\|\theta_i-\tilde{\theta}_j\right\|\right)^2}_{\text{virtual BSs}}+\underbrace{\sum_{i=1}^{q-1}\sum_{j>i}^{q}\frac{1}{\sigma_{ij}^{2}}\left(d_{ij}-\left\|\theta_i-\theta_j\right\|\right)^2}_{cooperation}\right\};q=2\sim M$$

(3.37)

where $\hat{\theta}_{s,q}=\left[\hat{\theta}_1 \quad \hat{\theta}_2 \quad \cdots \quad \hat{\theta}_q\right]^T$, $\tilde{\theta}_j$ denotes known position virtual BS. There are q unknowns of positions contained one target mobile and (q-*1*) auxiliary mobiles in (3.37) that is different from parallel method in (3.29). The complete algorithm of sequential pre-linear method is indicated in Figure 3.10.

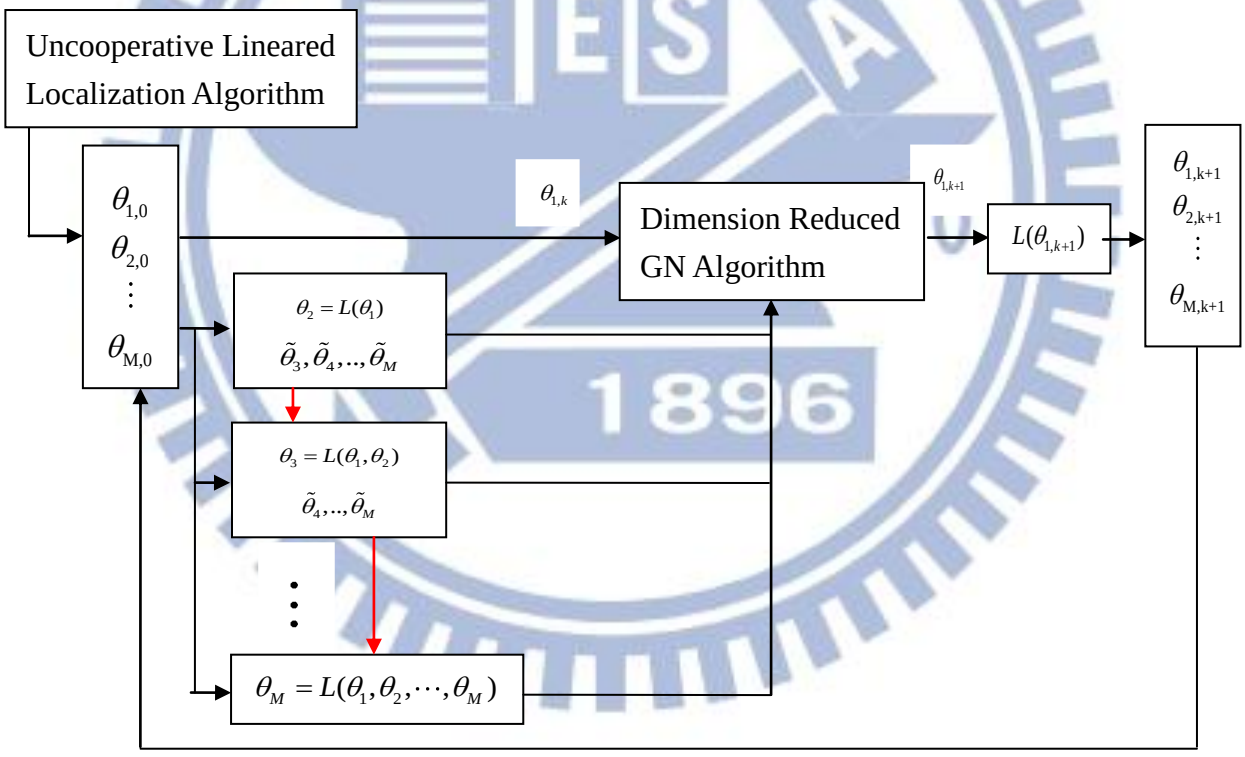

Figure 3.10 Sequential pre-linear algorithm

First, in the *k*th iteration, we focus on mobile 2. $\tilde{\theta}_{3,k-1}, \tilde{\theta}_{4,k-1}, .., \tilde{\theta}_{M,k-1}$ are virtual BSs which help mobile *2* to find the mapping function

$$\theta_{2,k} = g_{s\_2,k} + G_{s\_2,k}\theta_{1,k} . \qquad (3.38),$$

this is same as parallel pre-linear method in mobile *2*, i.e., $g_{s\_2,k} = g_{p\_2,k}; G_{s\_2,k} = G_{p\_2,k}$. After the mapping of mobile *2* is obtained, mobile *3* can be written as the function of target mobile and mobile *2* which is called virtual target, i.e., $\theta_3(\theta_1, \theta_2(\theta_1))$; based on the thought, mobile *M* can get the mapping of target mobile by using mobile *1* and other (*M-2*) virtual target respectively, i.e., $\theta_M(\theta_1, \theta_2(\theta_1), \theta_3(\theta_1), .., \theta_{M-1}(\theta_1))$. The linear TS equation in matrix form at the *k*th iteration can be written as

$$y_{s\_3,k} = J_{s\_3,k}\theta_{s\_3,k} + n_{s\_3,k} \qquad (3.39)$$

where $\theta_{s\_3,k} = \begin{bmatrix} \theta_{1,k} & \theta_{2,k} & \theta_{3,k} \end{bmatrix}^T$.

$$J_{s\_3,k} = \begin{bmatrix} J_{1,k} & 0 & 0 \\ v_{1,k} & 0 & 0 \\ 0 & J_{2,k} & 0 \\ 0 & v_{2,k} & 0 \\ 0 & 0 & J_{3,k} \\ 0 & 0 & v_{3,k} \\ h_{12,k}^T & -h_{12,k}^T & 0 \\ h_{13,k}^T & 0 & -h_{13,k}^T \\ 0 & h_{23,k}^T & -h_{23,k}^T \end{bmatrix} \qquad (3.40)$$

where $v_{j,k} = \begin{bmatrix} h_{j4,k} & h_{j5,k} & \cdots & h_{jM,k} \end{bmatrix}^T; j = 1,2,3$ denotes the virtual Jacobian matrix.

and

$$y_{s\_3,k} = \begin{bmatrix} y_{1,k} & y_{v_1,k} & y_{2,k} & y_{v_2,k} & y_{3,k} & y_{v_3,k} & y_{12,k} & y_{13,k} & y_{23,k} \end{bmatrix}^T$$

$$n_{s\_3,k} = \begin{bmatrix} n_{uncoop,1,k} & n_{coop,v_1,k} & n_{uncoop,2,k} & n_{coop,v_2,k} & n_{uncoop,3,k} & n_{coop,v_3,k} & n_{coop,12,k} & n_{coop,13,k} & n_{coop,23,k} \end{bmatrix}^T$$

(3.41)

where $y_{v_i,k}, n_{coop,v_i,k}$ are the terms related to mobile *i* and virtual BSs.

Denote $J_{s\_3,k} = \left[F_{s\_31,k} \quad F_{s\_32,k} \quad F_{s\_33,k} \right]$, (3.39) can be written as

$$(y_{s\_3,k} - F_{s\_31,k}\theta_{1,k} - F_{s\_32,k}\theta_{2,k}) = F_{s\_33,k}\theta_{3,k} + n_{s\_3,k} \qquad (3.42)$$

the LS estimator is given by

$$\theta_{3,k} = (F_{s\_33,k}{}^{T} W_{s\_3,k} F_{s\_33,k})^{-1} F_{s\_33,k}{}^{T} W_{s\_3,k} (y_{s\_3,k} - F_{s\_31,k}\theta_{1,k} - F_{s\_32,k}\theta_{2,k}) \qquad (3.43).$$

We can see that $\theta_{3,k}$ is written as function of $\theta_{1,k}$ and $\theta_{2,k}$. We insert (3.38) into (3.43), the mapping function between $\theta_{3,k}$ and target mobile is obtained as follows

$$\theta_{3,k} = g_{s\_3,k} + G_{s\_3,k}\theta_{1,k}$$

$$g_{s\_3,k} = \left(F_{s\_33,k}^{T} W_{s\_3,k} F_{s\_33,k} \right)^{-1} F_{s\_33,k}^{T} W_{s\_3,k} (y_{s\_3,k} - F_{s\_32,k} g_{s\_2,k})$$

$$G_{s\_3,k} = -\left(F_{s\_33,k}^{T} W_{s\_3,k} F_{s\_33,k} \right)^{-1} F_{s\_33,k}^{T} W_{s\_3,k} (F_{s\_31,k} + F_{s\_32,k} G_{s\_2,k}) \qquad (3.44).$$

where $W_{s\_3,k} = \left(E\left[n_{s\_3,k} n_{s\_3,k}^{T} \right] \right)^{-1}$ is diagonal weighting matrix. The location errors of virtual BSs will be discussed in Section 3.4.

Now mobile *3* transfers the function to target mobile successfully, the rest mobiles repeat the above procedure and the mapping function of mobile q in Figure 3.10 can be written as

$$g_{s\_q,k} = \left(F_{s\_qq,k}^{T} W_{s\_q,k} F_{s\_qq,k} \right)^{-1} F_{s\_qq,k}^{T} W_{s\_q,k} (y_{s\_q,k} - \sum_{j=2}^{q-1} F_{s\_qj,k} g_{s\_j,k}); q = 3 \sim M$$

$$G_{s\_q,k} = -\left(F_{s\_qq,k}^{T} W_{s\_q,k} F_{s\_qq,k} \right)^{-1} F_{s\_qq,k}^{T} W_{s\_q,k} (F_{s\_q1,k} + \sum_{j=2}^{q-1} F_{s\_qj,k} G_{s\_j,k}); q = 3 \sim M \qquad (3.45).$$

The mapping coefficients $g_{s\_q,k}$ and $G_{s\_q,k}$ are updated by iteration as before. The mapping is generated sequentially in each iteration, mapping function $L_{q,k}$ for sequential method needs the information of $L_{2,k} \sim L_{q-1,k}$ that is different from parallel pre-linear method. In next Section, the dimension-reduced GN algorithm is derived to solve the position of target mobile.

3.3 Dimension-Reduced GN Method of Target Mobile

The mapping functions of proposed three pre-linear methods are derived in previous Section. The next task is how to estimate the position of target mobile by using these mapping function. The dimension-reduced GN algorithm is derived based on GN method in Section 3.1.

In general, the size of mapping function g and G are same no matter what methods are used, so we denote the mapping function as

$$\theta_q = L_q(\theta_1) = g_q + G_q\theta_1 \qquad (3.46).$$

In (3.3), M unknown position coordinates are considered. According to (3.46), the original M unknown positions can be reduced to one unknown position. First, the uncooperative distance function (2.3) can be written as

$$B_{q\tilde{j}}(\theta_1) = \left\| g_q + G_q\theta_1 - BS_{\tilde{j}} \right\|, q = 2 \sim M, \tilde{j} = 1 \sim N \qquad (3.47),$$

Note that the term $B_{1\tilde{j}}(\theta_1) = \left\| \theta_1 - BS_{\tilde{j}} \right\|$ is same as the original model. The cooperative distance function (3.4) can be written as

$$B_{1q}(\theta_1, \theta_q) = \left\| (I - G_q)\theta_1 - g_q \right\|, q = 2 \sim M$$

$$B_{qj}(\theta_q, \theta_j) = \left\| (G_q - G_j)\theta_1 + (g_q - g_j) \right\|, q = 2 \sim M-1, j = q+1 \sim M \qquad (3.48)$$

The model has been changed to one position coordinate of mobile in (3.47) and (3.48). Then, the cost function (3.3) is given as

$$\hat{\theta}_1 = \min_{\theta_1} \left\{ \begin{array}{l} \underbrace{\sum_{\tilde{j}=1}^{N} \frac{1}{\sigma_{1\tilde{j}}^2} \left(d_{1\tilde{j}} - \left\| \theta_1 - BS_{\tilde{j}} \right\| \right)^2 + \sum_{q=2}^{M} \sum_{\tilde{j}=1}^{N} \frac{1}{\sigma_{q\tilde{j}}^2} \left(d_{q\tilde{j}} - \left\| g_q + G_q\theta_1 - BS_{\tilde{j}} \right\| \right)^2}_{Noncooperation} \\ + \underbrace{\sum_{i=2}^{M} \frac{1}{\sigma_{1q}^2} \left(d_{1q} - \left\| (I - G_q)\theta_1 - g_q \right\| \right)^2 + \sum_{q=2}^{M-1} \sum_{j=q+1}^{M} \frac{1}{\sigma_{qj}^2} \left(d_{qj} - \left\| (G_q - G_j)\theta_1 + (g_q - g_j) \right\| \right)^2}_{cooperation} \end{array} \right\}$$

(3.49)

The dimension-reduced GN method can solve (3.49). Apply Taylor-series expansion to (3.47) and (3.48) as follows

$$B_{q\tilde{j}}(\theta_1) = B_{q\tilde{j}}(\theta_{1,0}) + \partial B_{q\tilde{j}}^T \left(\theta_1 - \theta_{1,0}\right) + n_{B\_ts,q\tilde{j}}; q = 2 \sim M, \tilde{j} = 1 \sim N \qquad (3.50)$$

Note that the Taylor-series expansion of $B_{1\tilde{j}}(\theta_1)$ is same as the original model,

i.e., $\partial B_{1\tilde{j}} = J_{1\tilde{j}}; \tilde{j} = 1 \sim N$, and

$$B_{1q}(\theta_1) = B_{1q}(\theta_{1,0}) + \partial B_{1q}^T \left(\theta_1 - \theta_{1,0}\right) + n_{B\_ts,1q}, q = 2 \sim M$$

$$B_{qj}(\theta_1) = B_{qj}(\theta_{1,0}) + \partial B_{qj}^T \left(\theta_1 - \theta_{1,0}\right) + n_{B\_ts,qj}, q = 2 \sim M-1, j = q+1 \sim M \qquad (3.51)$$

where n_{B_ts} denotes the higher order truncation error vector of Taylor approximation, and the gradient vector

$$\partial B_{q\tilde{j}}^T = \frac{(g_q + G_q\theta_1 - BS_{\tilde{j}})^T}{B_{q\tilde{j}}(\theta_{1,0})} G_q, q = 2 \sim M, \tilde{j} = 1 \sim N$$

$$\partial B_{1j}^T = \frac{((I - G_j)\theta_1 - g_j)^T}{B_{1j}(\theta_{1,0})}(I - G_j), j = 2 \sim M$$

$$\partial B_{qj}^T = \frac{((G_q - G_j)\theta_1 + (g_q - g_j))^T}{B_{qj}(\theta_{1,0})}(G_q - G_j), q = 2 \sim M-1, j = q+1 \sim M \qquad (3.52)$$

Contrast with the original model, the terms G_q, $(I - G_q)$ and $(G_q - G_j)$ in (3.52) are the revised terms which adjust the gradient vector between mobile *q* and BSs, target mobile, mobile *j*, respectively. It is different from original GN algorithm since the mapping functions are considered to reduce the dimension to avoid the $3M \times 3M$ matrix inversion. In case *M=4*, dimension-reduced TS matrix equation is given by

$$d = B(\theta_{1,0}) + \partial B(\theta_1 - \theta_{1,0}) + n_{rGN} \qquad (3.53)$$

where

$$\partial B = \begin{bmatrix} J_1^T & \partial B_2^T & \partial B_3^T & \partial B_4^T & \partial B_{12} & \partial B_{13} & \partial B_{14} & \partial B_{23} & \partial B_{24} & \partial B_{34} \end{bmatrix}^T$$

$$\partial B_q = \left[\partial B_{q\tilde{1}} \quad \partial B_{q\tilde{2}} \quad \partial B_{q\tilde{3}} \quad \partial B_{q\tilde{4}} \right]^T$$

(3.54)

$$B(\theta_1) = \left[A_1^T \quad B_2^T \quad B_3^T \quad B_4^T \quad B_{12} \quad B_{13} \quad B_{14} \quad B_{23} \quad B_{24} \quad B_{34} \right]^T$$

$$B_q = \left[B_{q\tilde{1}} \quad B_{q\tilde{2}} \quad B_{q\tilde{3}} \quad B_{q\tilde{4}} \right]^T$$

(3.55)

$$n_{rGN} = n_{B\_ts} + n_{ts} \qquad (3.56)$$

The only different term between n_{rGN} and $\underline{n}$ in (3.7) is the Taylor high order truncation error n_{B_ts} and n_{ts}. According to (3.53), the objective function is denoted as

$$\hat{\theta}_1 = \arg\min_{\theta_1} \left\| d - B(\theta_{1,0}) - \partial B(\theta_1 - \theta_{1,0}) \right\|_{W_r}^2 \qquad (3.57)$$

and the dimension-reduced GN estimator solve (3.57) iteratively by

$$\hat{\theta}_{1,k+1} = \hat{\theta}_{1,k} + (\partial B_k{}^T W_{r,k} \partial B_k)^{-1} \partial B_k{}^T W_{r,k} (d - B(\theta_{1,k})) \qquad (3.58)$$

where the $W_{r,k}$ is covariance inverse of $n_{rGN,k}$,

$$W_{r,k} = \left(E\left[n_{rGN,k} n_{rGN,k}^T \right] \right)^{-1}$$

$E\left[n_{rGN,k} n_{rGN,k}^T \right]$ is a diagonal matrix with variance of Taylor truncation error and measurement noise.

After θ_1 is updated, the auxiliary mobiles can be obtained by the pre-linear mapping function which is generated at step 1. We note that target mobile affect the accuracy of auxiliary mobiles. The choice of target mobile is another issue and will be discussed in Section 3.5. However, estimate of the target mobile still suffers location error, and it can affect the accuracy of auxiliary mobiles. The location errors of target mobile and virtual BSs will be discussed and compensated in Section 3.4.

3.4 Weighting Compensation in Inaccurate Cooperative Mobiles

The position uncertainty is known to degrade the localization accuracy [21]. The pre-linear method in Section 3.2, virtual BSs with uncertain position are utilized to estimate the position of mobiles, the presence of location error may degrade the performance in location estimation. [21] derived the variance of uncertain sensor error. In cooperative system, the effect on location errors of uncertain positions of virtual BSs can be derived based on [21].

The cooperative measurement model between mobile *i* and mobile *j* is given by

$$d_{ij} = \left\| \theta_i - \theta_j \right\| + n_{ij} \qquad (3.59)$$

In (3.59), the position of mobile *i* and mobile *j* are estimated jointly. If the uncertain position coordinate of mobile *j* is gotten, mobile *j* is a virtual BS to mobile *i* and (3.59) can be written as

$$d_{ij} = \left\| \theta_i - \tilde{\theta}_j + e_j \right\| + n_{ij} \qquad (3.60)$$

where $e_j \in R^{3,1}$ is the location error which is denoted in (3.34). Compared with (3.29) and (3.37), the location error e_j in (3.60) is inside the norm; if the error term can get out of the norm function, the virtual measurement model between mobile *i* and virtual BS *j* is obtained. Therefore, we apply Taylor-series expansion to (3.60) as follows

$$d_{ij} = \left\| \theta_i - \tilde{\theta}_j \right\| + h_{ij}^T e_j + \text{higher order terms} + n_{ij} \qquad (3.61)$$

where $h_{ij} = \dfrac{(\theta_i - \tilde{\theta}_j)}{\left\| \theta_i - \tilde{\theta}_j \right\|}$ is the gradient vector between mobile *i* and virtual BS *j*.

Assume that the higher order term is neglected due to the good reference point, (3.61) can be written as

$$d_{ij} = \left\| \theta_i - \tilde{\theta}_j \right\| + h_{ij}^T e_j + n_{ij} \qquad (3.62)$$

In (3.62), the location error is out of the norm function and the total error includes virtual BS

error $h_{ij}^T e_{v\_j}$ and measurement noise n_{ij}. The variance of total error is

$$\sigma_{T\_ij}^2 = E\left[\left(h_{ij}^T e_j + n_{ij}\right)^2\right] \qquad (3.63)$$

We assume that the measurement noise and virtual BS error are independent, then (3.63) can be written as

$$\sigma_{T\_ij}^2 = \sigma_j^2 + \sigma_{ij}^2 \qquad (3.64)$$

where $\sigma_j^2 = h_{ij}^T \operatorname{cov}(e_j) h_{ij}$.

Actually, the covariance matrix of virtual BS error is hard to derive. We simply use the result of (2.15) in our algorithm, and an example is given in parallel pre-linear method. Based on (2.15), it is assumed that the virtual BS errors are i,i,d. The covariance matrix of e_j can be written according to (3.36) as follow

$$\operatorname{cov}(e_j) = (diag(F_{p\_j2}^T W_{p\_j} F_{p\_j2}))^{-1} \qquad (3.65)$$

The error variance of virtual BSs $\sigma_{v\_j}^2$ is smaller and smaller by iteration since the position of virtual BS becomes more accurate.

On the other hand, the position of target mobile can affect the accuracy of auxiliary mobiles. If the position of target mobile is given, the corresponding auxiliary mobile *i* can be obtained by the mapping function. The location error of target mobile *1*, $e_1 = \hat{\theta}_1 - \theta_1 \in R^3$, is involved in localization by the inner product with h_{1j}^T, which is similar to virtual BSs, i.e., $\sigma_{e_{1j}}^2 = h_{1j}^T \operatorname{cov}(e_1) h_{1j}$. The variance of total error in target mobile *1* and auxiliary mobile *j* is

$$\sigma_{Total\_1j}^2 = \sigma_{e_{1,j}}^2 + \sigma_{1j}^2,\ j = 2 \sim M \qquad (3.66)$$

Assuming that the location error of target mobile is i.i.d, the covariance matrix of e_1 can be written according to (3.58) as follows

$$\mathrm{cov}(e_1) = (diag(\partial B^T W_r \partial B))^{-1} \qquad (3.67)$$

By iteration, $\sigma_{e_{1i}}^2$ is smaller because of the accurate target mobile.

The weighting compensation on target mobile error improves the accuracy of mapping function in all algorithms in Section 3.2, while the virtual BSs errors are applied in parallel and sequential methods. We note that the target mobile error and virtual BSs error can be combined together to enhance the localization accuracy. The performance is improved as seen by computer simulation.

3.5 Target Mobile Selection

In fact, we know that the choice of mapping function is unlimited that is mentioned in Section 3.2. In pre-linear methods, the position coordinates of auxiliary mobiles are written as the linear function of target mobile, i.e., $\theta_q = L_q(\theta_1)$. Actually, the true position of target mobile is unknown, so the mapping includes the location error of target mobile. How to choose a probable target mobile is an important issue since the target mobile also affects the convergence and the RMSE which are shown in simulations. In [23], the reference selection on hyperbolic-canceled linear algorithm is proposed to select the reference by using the minimum measurement. Here, the target mobile selection scheme is based on [23].

The reliability of measurements and positions of mobile affect the performance of localization; we believe that the small measured distance is reliable contrast to the large measured distance. A simple method for target mobile selection is to choose the mobile with the smallest square measurement from fixed BS and other mobiles, the mathematical expression is given as follow

$$mobile_i = \min_i \sum_{\tilde{j}=1}^{N} d_{i\tilde{j}}^2 + \sum_{j=1, j\neq i}^{N} d_{ij}^2 \qquad (3.68)$$

where $d_{i\tilde{j}}$ and d_{ij} are measured distance from mobile *i* to BS $\tilde{j}$ and mobile *j*, respectively. According to (3.68), mobile *i* is selected as target mobile. In Section 4.3, simulations validate that the target mobile selection scheme is useful to improve the performance.

3.6 Computation Cost

In this section, the computation cost of three pre-linear methods in Section 3.2 and dimension-reduced GN method in Section 3.3 are compared with joint GN algorithm. The total numbers of multiplications in each iteration are computed as the complexity evaluation. Here, the 3-D space is considered with *N* fixed BSs and *M* unknown positions of mobiles.

(a). Joint GN method

First, the computation load of joint GN algorithm comes from (3.10), we rewrite (3.10) as follows

$$(J^T W J)(\hat{\theta}_{k+1} - \hat{\theta}_k) = J^T W (d - A(\theta_k)) \qquad (3.69)$$

From (3.69), there are two parts of computation that include the matrix multiplication part among matrix and updating part $J, A(\theta_k)$. The weighting matrix W is assumed to be an identity matrix for simplicity. The detail multiplication is given as follows

1. $$J^T J = \begin{bmatrix} J_1^T J_1 + \sum_{j=2}^{M} h_{1j} h_{1j}^T & -h_{12} h_{12}^T & \cdots & -h_{1M} h_{1M}^T \\ -h_{12} h_{12}^T & J_2^T J_2 + \sum_{\substack{j=1 \\ j\neq 2}}^{M} h_{2j} h_{2j}^T & \cdots & -h_{2M} h_{2M}^T \\ \vdots & \vdots & \ddots & \vdots \\ -h_{1M} h_{1M}^T & -h_{2M} h_{2M}^T & \cdots & J_M^T J_M + \sum_{j=1}^{M-1} h_{Mj} h_{Mj}^T \end{bmatrix}_{3M \times 3M} \qquad (3.70)$$

where $J_i \in R^{N\times 3}, h_{ij} \in R^{3\times 1}$. The multiplication include total $9NM$ for $J_i^T J_i, i = 1 \sim M$, and $9 \times C(M,2)$ for $h_{ij} h_{ij}^T$.

2. $$J^T \times \underbrace{(\underline{d} - A(\theta_k))}_{s} = \begin{cases} J_1^T s_1 + \sum_{j=2}^{M} h_{1j} s_{1j} \\ J_2^T s_2 + \sum_{\substack{j=2 \\ j\neq 1}}^{M} h_{2j} s_{2j} \\ \vdots \\ J_M^T s_M + \sum_{j=1}^{M-1} h_{Mj} s_{Mj} \end{cases} \qquad (3.71)$$

$J_i^T x_i, i = 1 \sim M$ requires $3NM$,and $3 \times C(M,2)$ for $h_{ij} s_{ij}$

3. The explicit computation of the inverse of the $(J^T J)$ is avoided by applying Cholesky decomposition [24], i.e., $(J^T J) = LL^T$, which requires $(3M)^3$.

4. To generate $(\hat{\theta}_{k+1} - \theta_k)$ from $LL^T \times (\hat{\theta}_{k+1} - \theta_k)$, it needs $(3M)^2 + 3M$.

5. The updating terms $J_i \in R^{N\times 3}, h_{ij} \in R^{3\times 1}$ need *1* division in every element, so requiring $3NM + 3 \times C(M,2)$ in total. The distance vector $A(\theta_k)$ contains an inner product and one division in every element, so total $4(NM + C(M,2))$ are needed.

The total multiplication for joint GN method is $19(MN + C(M,2)) + 27M^3 + 9M^2 + 3M$.

(b). Dimension-Reduced GN method of target mobile

The computation of dimension-reduced GN method is as follows

$$(\partial B^T \partial B)(\hat{\theta}_{1,k+1} - \hat{\theta}_{1,k}) = \partial B^T (d - B(\theta_{1,k})) \qquad (3.72)$$

where $\partial B \in R^{(MN+C(M,2))\times 3}$.

1. $\partial B^T \partial B \in R^{3\times 3}$ requires $9(MN + C(M,2))$.

2. $\partial B^T \times (d - B(\theta_{1,k})) : 3(MN + C(M,2))$

3. Cholesky decomposition: $(J^T J) = LL^T : 3^3$

4. $(\hat{\theta}_{k+1} - \theta_k) : 3^2 + 3 = 12$

5. The updating terms is same as joint GN method.

6. The different term from joint GN method is that (3.52) includes revised term G in each

row except the first block in ∂B that requires $9((M-1)N+C(M,2))$.

(c). Joint pre-linear method

The calculations of joint pre-linear mapping function is given as

$$(F^T F)\theta_k' = F^T(y - F_1\theta_{1,k})$$

$$(F^T F)g_{joint} = F^T y \in R^{3*(M-1),1}$$

$$(F^T F)G_{joint} = -F^T F_1 \in R^{3(M-1)\times 3(M-1)} \quad (3.73)$$

The terms g_{joint} and G_{joint} should be calculated individually since G_{joint} is used in the dimension-reduced GN method. The term $F^T F$ can be written as follows

$$F^T F = \begin{bmatrix} J_2^T J_2 + \sum_{\substack{j=1 \\ j\neq 2}}^{M} h_{2j} h_{2j}^T & -h_{23}h_{23}^T & \cdots & -h_{2M}h_{2M}^T \\ -h_{23}h_{23}^T & J_3^T J_3 + \sum_{\substack{j=1 \\ j\neq 3}}^{M} h_{3j} h_{3j}^T & \cdots & -h_{3M}h_{3M}^T \\ \vdots & \vdots & \ddots & \vdots \\ -h_{2M}h_{2M}^T & -h_{3M}h_{3M}^T & \cdots & J_M^T J_M + \sum_{j=1}^{M-1} h_{Mj} h_{Mj}^T \end{bmatrix}_{3(M-1)\times 3(M-1)} \quad (3.74)$$

The cost in $F^T F$ is same as the lower-right $3(M-1)\times 3(M-1)$ sub-block of (3.70). and $F^T y$ is same as the sub-block of (3.71). We can see that the total cost in g_{joint} is similar to joint GN method with $M \to (M-1)$. On the other hand, the inverse of matrix of G_{joint} is same as g_{joint}; the additional calculations in term G_{joint} is generating G_{joint} with triangular matrix multiplication: $3((3(M-1))^2 + 3(M-1))$. However, according to the term $F^T F_1 = \begin{bmatrix} h_{12}h_{12}^T \\ h_{13}h_{13}^T \\ \vdots \\ h_{1M}h_{1M}^T \end{bmatrix} \in R^{(M-1)\times 3}$, we can see that there is no need to compute $F^T F_1$ since the sub-block $h_{1i}h_{1i}^T$ is obtained from (3.74).

(d). Parallel pre-linear method

Same as joint method, the mapping function g_{p_q} and G_{p_q} should be

calculated individually. The term $F_{p\_q}{}^T F_{p\_q} = J_q^T J_q + \sum_{\substack{j=1 \\ j\neq q}}^{M} h_{qj} h_{qj}^T; q = 2 \sim M$ is equal to the diagonal block of (3.102). The total cost in g_{p_q} include the first and second terms in joint GN method with $M \to (M-1)$, $3^3(M-1)$ for Cholesky decomposition and $(3^2+3)(M-1)$ for generating g_{p_q}. Same as joint method, the additional computation for G_{p_q} is $3(3^2+3)(M-1)$.

(e). Sequential pre-linear method

We know that the sequential method and parallel method are same in mapping function of mobile *2*. Compared with (3.36) and (3.45), the only difference between parallel and sequential method is that $\sum_{j=2}^{q-1} F_{s\_qj,k} g_{s\_j,k}$ in $g_{s\_q,k}$ and $\sum_{j=2}^{q-1} F_{s\_qj,k} G_{s\_j,k}$ in $G_{s\_q,k}$. Compared with parallel method, the additional $12C(M-1,2)$ multiplication is needed.

Table 3.1 compare the difference between joint GN and proposed methods. Note that the total computation cost in our methods includes pre-linear method in step 1 and dimension-reduced method in step 2.

Table 3.1 compare the difference between joint GN and proposed methods. Note that the total computation cost in our methods includes pre-linear method in step 1 and dimension-reduced method in step 2.

	GN	joint	parallel	sequential	DR-GN
1. $J^T \times J$	$9(MN + C(M,2))$	$M \to M-1$	$M \to M-1$	$M \to M-1$	M
2. $J^T \times (\underline{d} - A(\theta_k))$	$3(MN + C(M,2))$	$M \to M-1$	$M \to M-1$	$M \to M-1$	M
3. $(J^T J) = LL^T$	$\frac{1}{3}(3M)^3$	$M \to M-1$	$\frac{3^3}{3}(M-1)$	$\frac{3^3}{3}(M-1)$	$\frac{3^3}{3}$
4. LU	$3M^2 + 3M$	$M \to M-1$	$(3^2+3)(M-1)$	$(3^2+3)(M-1)$	3^2+3
5. J_k, A_k	$7(MN + C(M,2))$	$M \to M-1$	$M \to M-1$	$M \to M-1$	M
6. G	X	$3((3(M-1))^2 + 3(M-1))$	$3(3^2+3)(M-1)$	$3(3^2+3)(M-1)$	X
7. $\partial B \times G$	X	X	X	X	$9(MN + C(M,2))$

Table 3.1 Comparison of computation for joint GN method and prelinear methods

The dominate term in joint GN and joint per-linear method is Cholesky decomposition, which need roughly M^3 computation. In parallel, sequential and DR-GN mehods, the term can be reduced to $\frac{3^3}{3}(M-1)$. On the other hand, the terms 1, 2, 4 and 5 in DR-GN method equals to joint GN method, so computation in these terms needs additional cost. The term 6 and 7 involve the computation of mapping function, which is no need in joint GN method.

Table 3.2 summarizes the total costs in joint GN method and three pre-linear methods

algorithms	Number of multiplications per iteration
GN	$9M^3 + 19M^2 + 19NM - 16M$
joint	$9M^3 + 33M^2 + 47NM - 88M - 28N + 39$
parallel	$24M^2 + 47NM + 13M - 38N + 40$
sequential	$30M^2 + 47NM - 5M - 38N + 52$

Table 3.2 Total computation cost

From Table 3.2, we can see that the major multiplication $9M^3$ in GN method and joint method caused by the inverse matrix in (3.10) and (3.22). The different between joint GN and joint method is that the dimension of inverse matrix is $3M \times 3M$ in GN method, while $3(M-1) \times 3(M-1)$ in joint method, but the total cost is higher than joint GN by $14M^2$ when *M*>>*N* due to the extra cost in dimension-reduced GN and computation in G. However, in parallel and sequential method, the dimension of inverse matrix in (3.36) and (3.45) is 3×3, this is why there is no M^3 terms in total multiplication and total cost is reduced greatly. We conclude that parallel and sequential methods reduce the cost successfully.

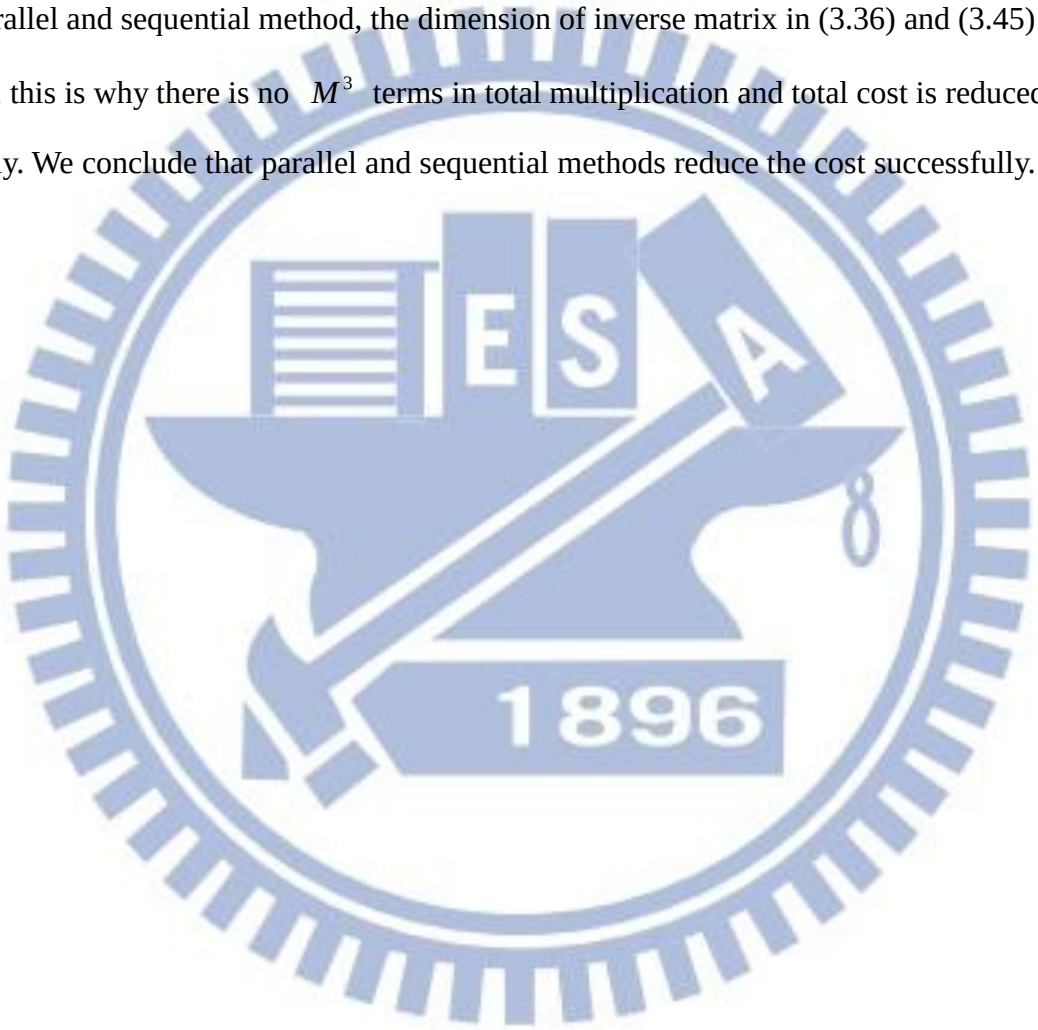

Chapter 4
Computer Simulations

In this Chapter, computer simulations show the performance of methods we proposed. In Section 4.1, we compare three pre-linear methods which are mentioned in Section 3.2 with joint GN method and CRLB. In Section 4.2, we show that how the reliability of measurements affects the localization accuracy. Section 4.3 shows the target mobile selection scheme helps to improve the accuracy and convergence. In Section 4.4, the effects on weighting including noise variance, Taylor modeling error and the compensation of virtual BSs and target mobile are shown.

The performance measure for localization evaluation is Root Mean Square Error (RMSE) which is denoted as

$$rmse = \sqrt{\frac{1}{500}\sum_{k=1}^{500}\left(\frac{\left\|\hat{\theta}_k - \theta\right\|^2}{M}\right)} \qquad (5.1)$$

where $\hat{\theta}_k$ is the estimate in the *k*th trial, *M* is the number of mobiles as before and 500 independent trials are run. Here, noise is AWGN and standard deviation (std) of measurements are based on [13],

$$\sigma_{ij} = 0.016(0.64\exp(-\alpha/0.6)A_{ij}^{1.5} + 1) \qquad (5.2)$$

The noise variance is affected by the true distance between mobile *i* and BS $\tilde{j}$ (or mobile *j*) and α is an adjustable coefficient. However, the true distance is not known in practice; the real distance A_{ij} in (5.2) is replaced by the measurement distance d_{ij} in simulations. We note that even only the 3-D environment is mentioned in previous Chapters, our simulations present both 2-D and 3-D cases, and the geometries are as follow

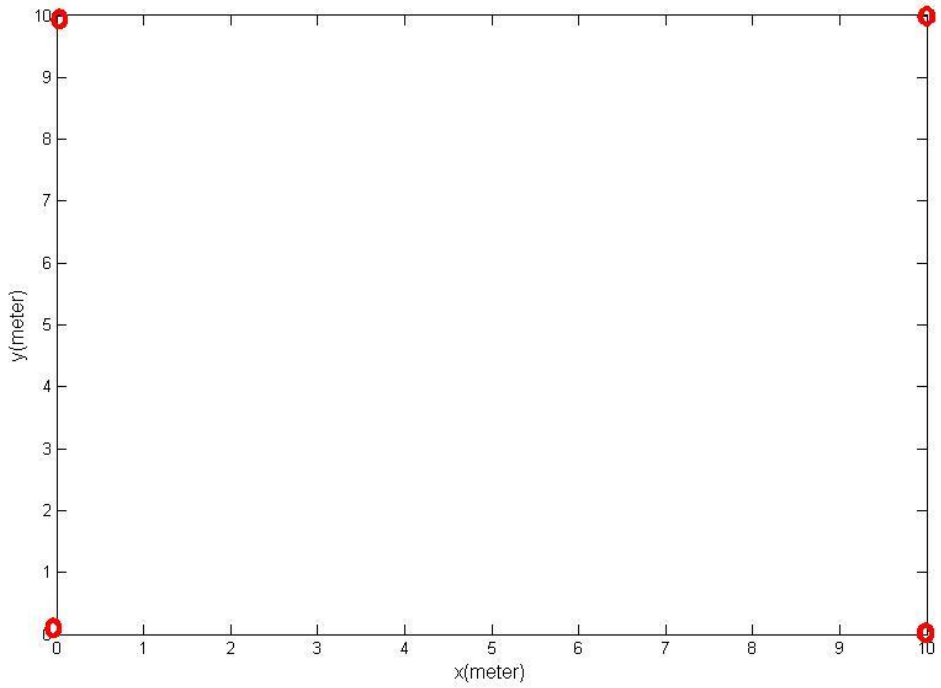

Figure 4.1 2-D geometry

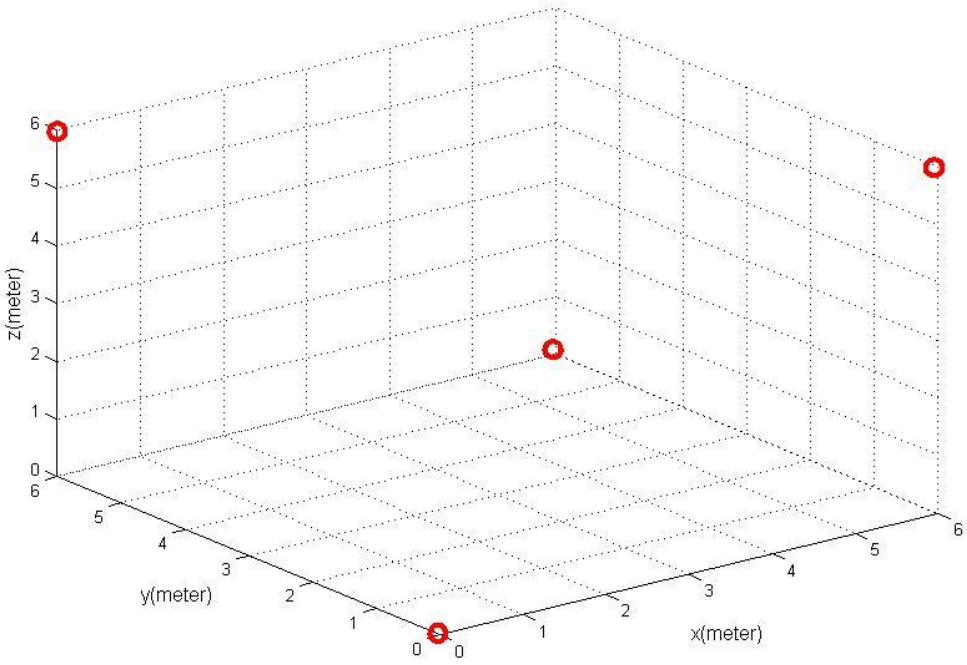

Figure 4.2 3-D geometry

BSs are placed at [0 0], [10 0], [0 10] and [10 10] in 2-D case, [0 0 0], [6 6 0], [6 0 6] and [0 6 6] in 3-D case. Mobiles are randomly selected within the geometry.

4.1 The Comparison of Pre-Linear Methods and Joint-GN method

We compare the RMSE to CRLB in cooperative localization in Section 4.1.1. Then, in cooperative scheme, the proposed pre-linear methods are compared with the joint GN method in Section 4.1.2.

4.1.1 The Comparison to CRLB

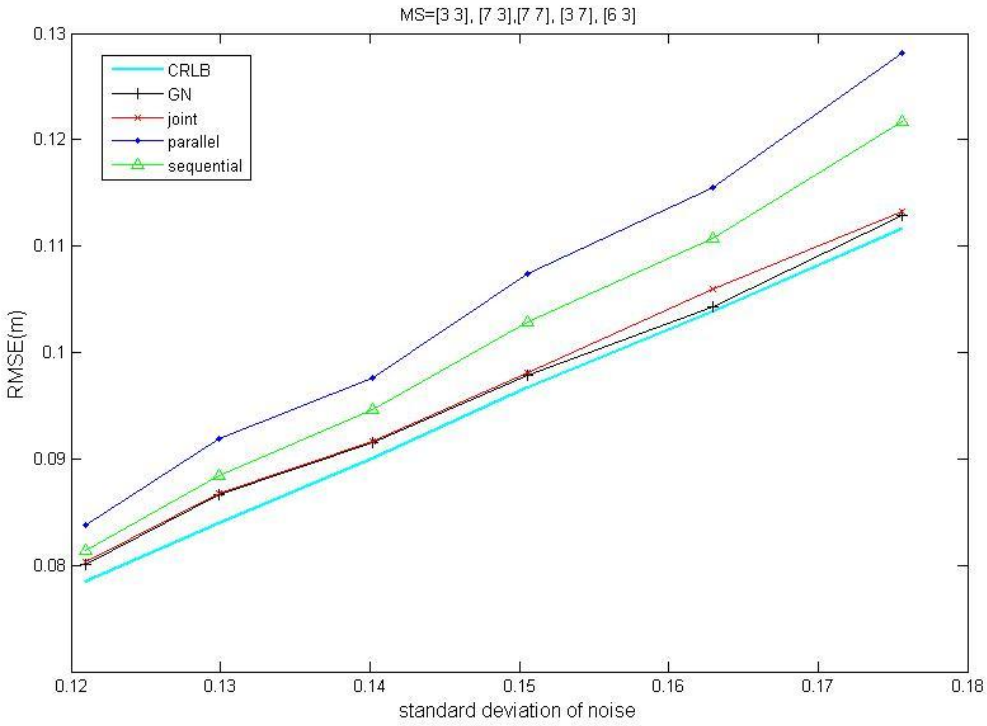

Figure 4.3 RMSE versus noise variance for pre-linear methods and GN method with CRLB in 2-D case

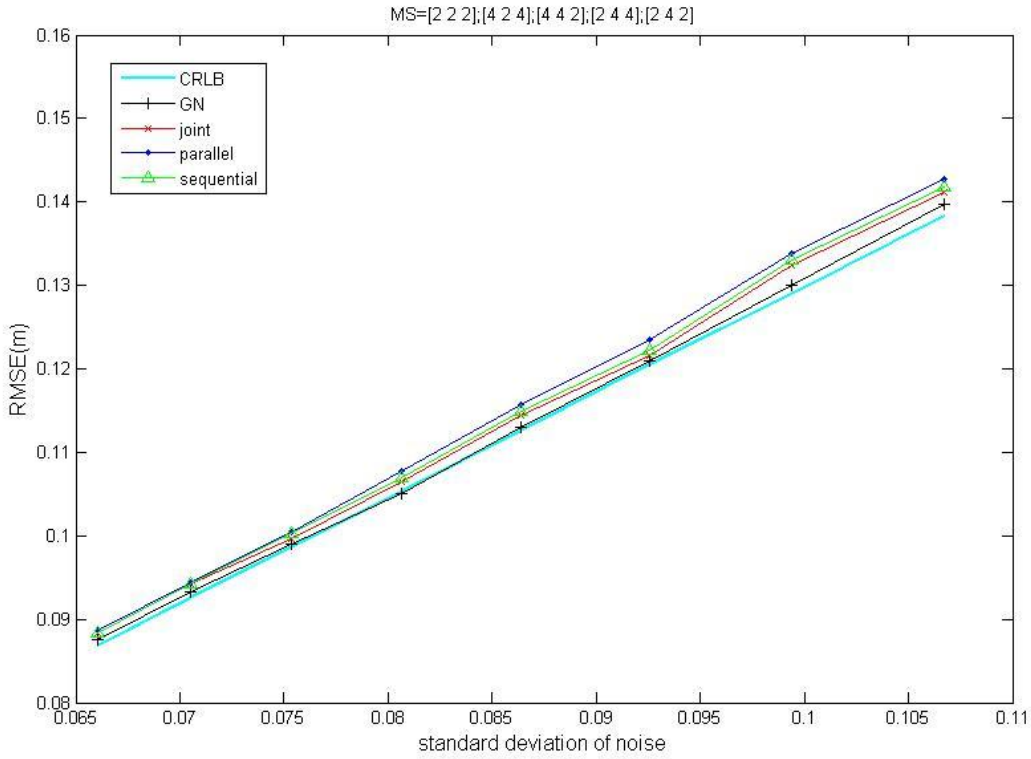

Figure 4.4 RMSE versus noise variance for pre-linear methods and GN method with CRLB in 3-D case

From Figure 4.3 and 4.4, joint GN method in (3.10) is very close to CRLB (3.14) noth in 2-D and 3-D case, but its high computation load is sacrificed. The RMSE of joint pre-linear method is better than parallel and sequential methods and approaches to joint GN method. On the other hand, sequential method is better than parallel method because the estimated positions are close to the true positions. For example in M=3 for sequential method, when $\theta_{1,k+1}$ is updated, it is used to locate the position of $\theta_{2,k+1}$, and the updated $\theta_{1,k+1}$ and $\theta_{2,k+1}$ are used to locate the position of $\theta_{3,k+1}$; while the parallel method only use the *k-th* position of mobiles. We believe that the updated position is useful in our simulation so that the performance will be enhanced in sequential method.

.

4.1.2 Comparison of Pre-Linear Methods and Joint-GN method

In this Section, convergence and effect on number of mobiles are considered. In Figure 4.5, the convergence rate is considered.

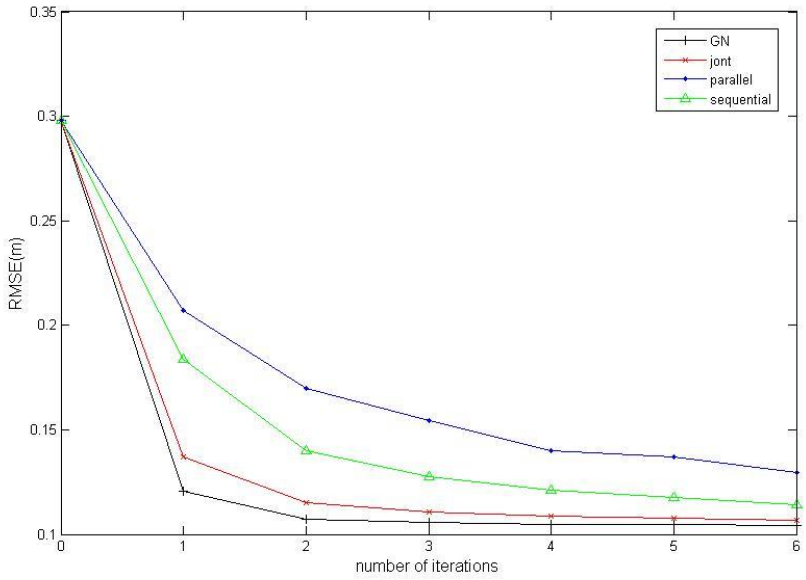

(a)

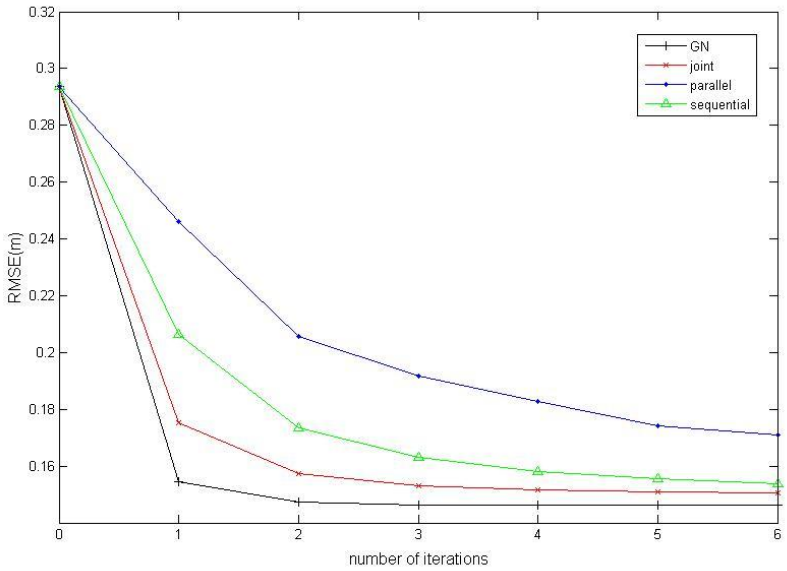

(b)

Figure 4.5 RMSE vs. convergence rate for pre-linear methods and joint GN method in (a) 2-D case (b) 3-D case

In Figure 4.5, six mobiles are considered. We can see that joint method and GN method need two iterations to converge both in 2-D and 3-D case, while sequential and parallel are about 5.

In the following figure, divided method for Jacobi and Gauss-Seidel methods mentioned in Section 3.1.2 are compared to parallel and sequential methods in 3-D case. Note that parallel and sequential methods use the additional mapping information between target and auxiliary mobiles while Jacobi and Gauss-Seidel method regard the other mobiles as virtual BSs with known position. The number of mobiles is set to 3 and randomly located in $6\times6\times6$ geometry.

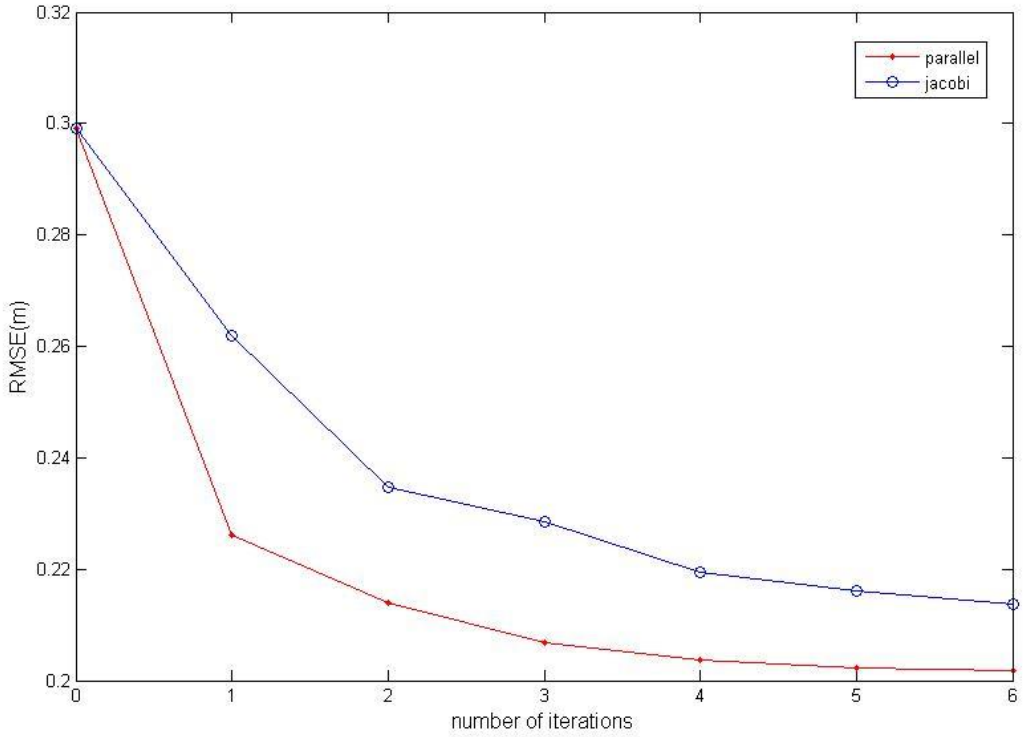

(a)

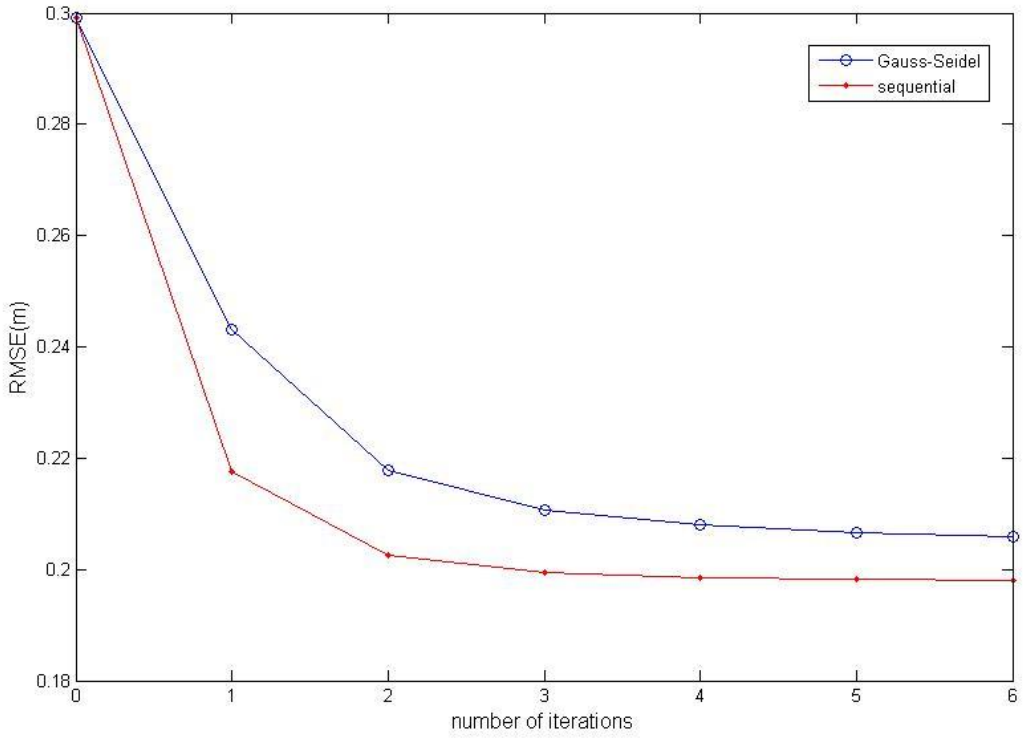

(b)

Figure 4.6 RMSE vs. convergence rate for (a) parallel method and Jacobi method (b) sequential and Gauss-Seidel method in 3-D case

Figure 4.6 compares proposed parallel and sequential methods with Jacobi and Gauss-Seidel method respectively. We can see that parallel method is better than Jacobi method in Fig 4.6 (a) and sequential method is better than Gauss-Seidel method in Fig 4.6 (b). This simulation shows that the transformed mapping functions in parallel and sequential methods are useful to improve the accuracy of positions. However, the extra computation cost is needed for parallel and sequential methods.

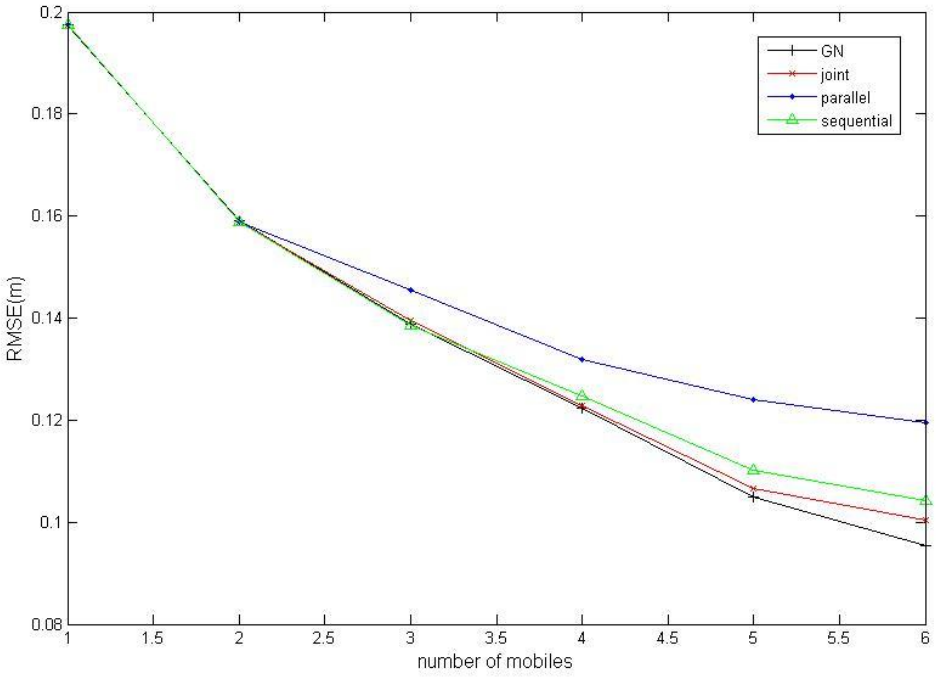

(a)

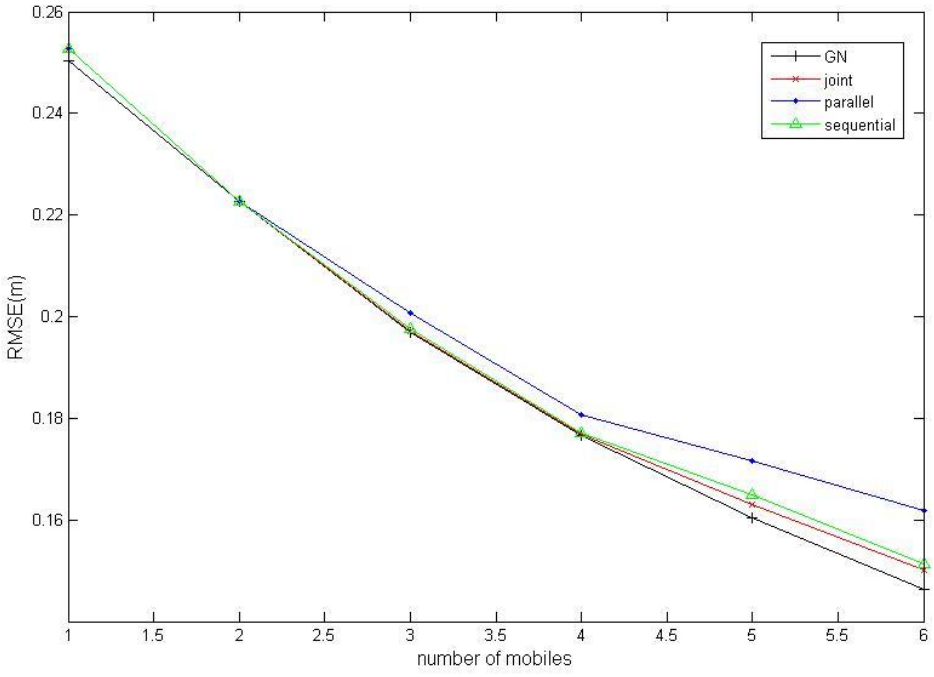

(b)

Figure 4.7 RMSE vs. the number of mobiles for pre-linear methods and GN method in (a) 2-D (b) 3-D case

In (3.3), we expect that the cooperative terms can improve the localization accuracy because of the information exchange between mobiles. Number of mobile from 2 to 6 is set in our simulation. From Figure 4.7, the RMSE improves when the number of mobiles increases. The worst RMSE occurs in number of mobiles equals to one, which means uncooperative localization. However, the quality of the cooperative information is important, or the localization accuracy may be degraded, which will be discussed in Section 4.2.

4.2 The Reliability of Cooperative Localization

We take two factors of cooperative localization into consideration in this Section. The discussion of noise variance of cooperative measurements is given in Section 4.2.1. The reliability of positions of mobiles is discussed in Section 4.2.2.

4.2.1 Measurement between Mobiles

We explore the cooperative localization when mobiles are in noisy channel. The measured distance is affected by measured noise, i.e., $d_{ij} = A_{ij} + n_{ij}$ .The noise variance of measurement between mobile *i* and mobile *j* σ_{ij}^2 in (3.1) affects the accuracy of localization. The simulation setup is as follows

The noise variances of uncooperative measurements are based on (4.2) with α set to 0.3. we The cooperative measurements are set with the factor α equals to 0.5 (reliable) and 0.1 (unreliable), respectively. We expect that the reliable cooperative measurements can improve the accuracy of position. The simulation results compare CDF (Cumulative Density Function) which are given in Figure 4.8 to Figure 4.10.

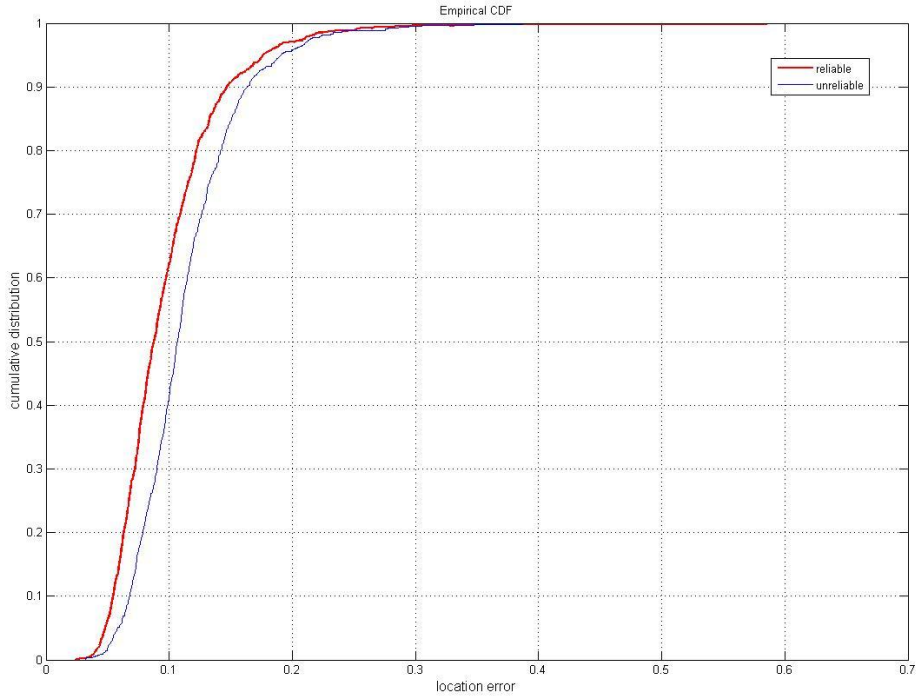

(a)

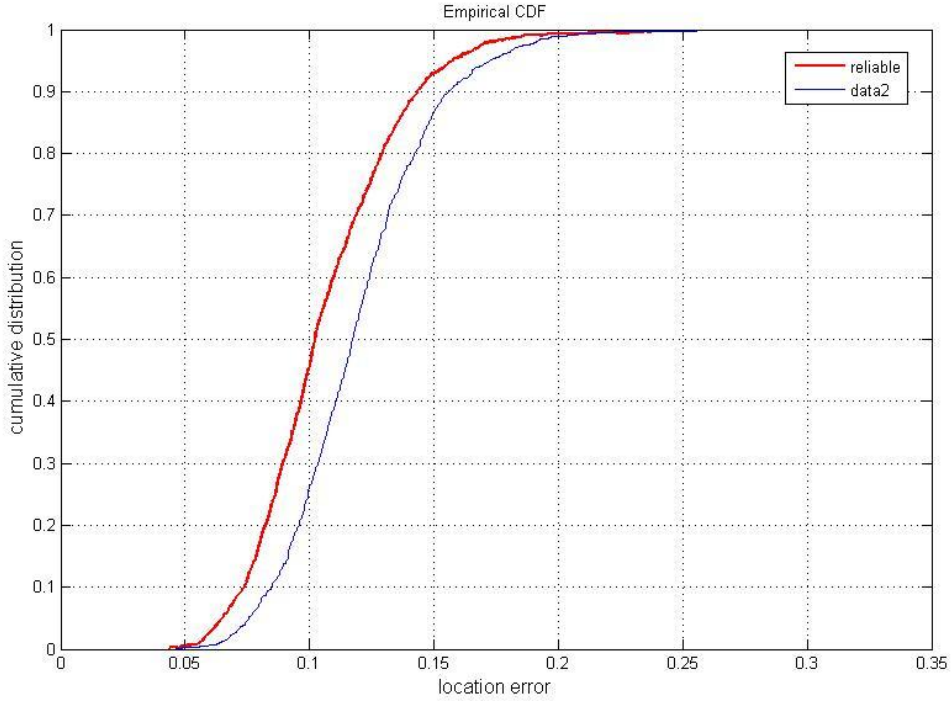

(b)

Figure 4.8 Comparison of CDF of location error for joint pre-linear method in (a) 2-D (b) 3-D case

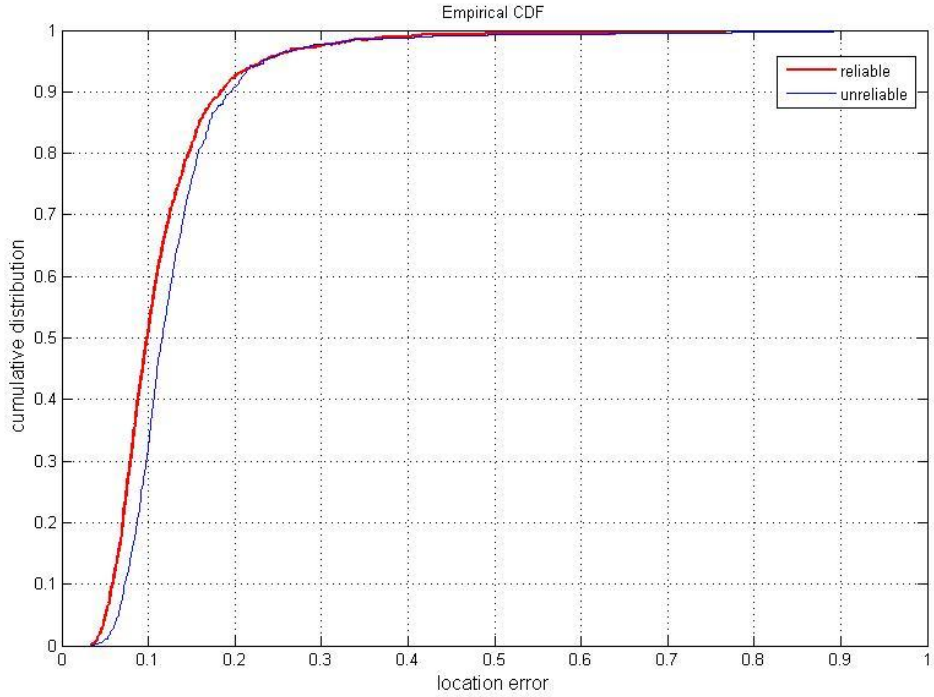

(a)

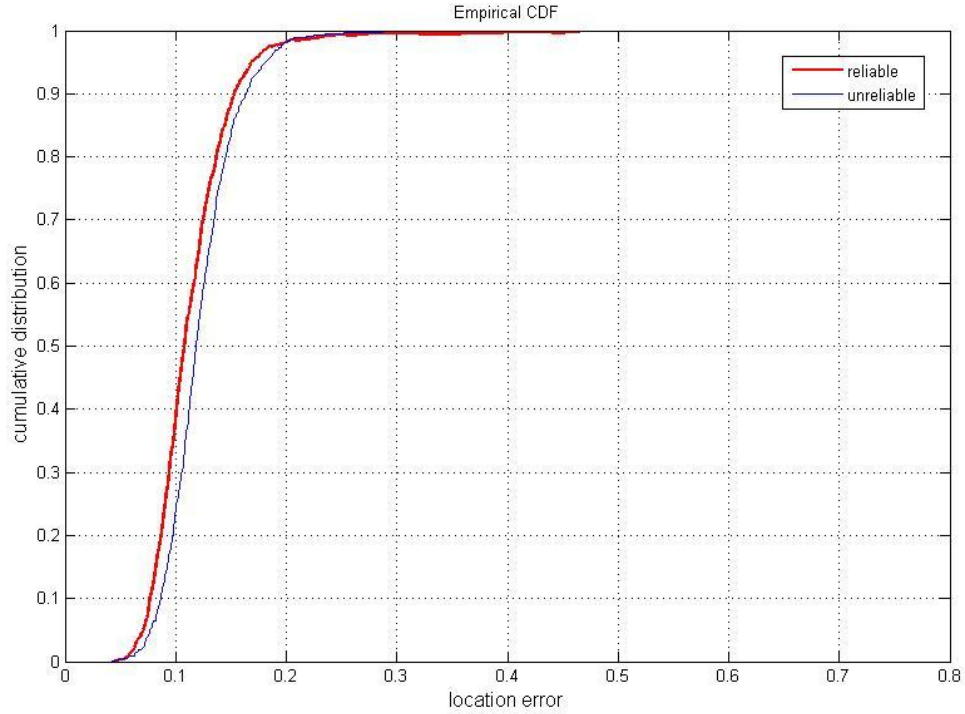

(b)

Figure 4.9 Comparison of CDF of location error for parallel pre-linear method in (a) 2-D (b) 3-D case

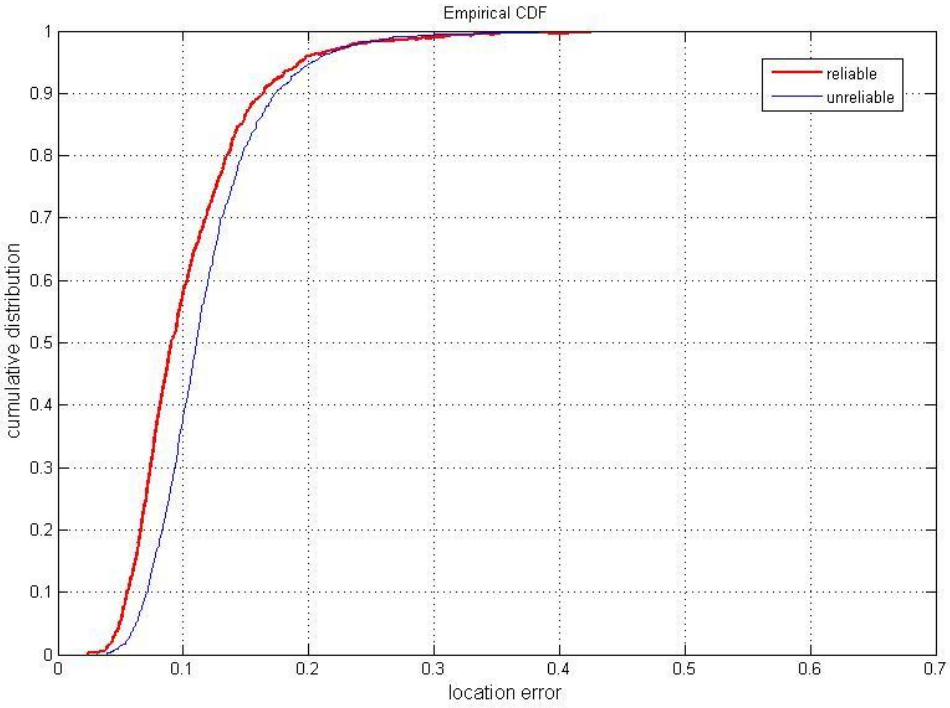

(a)

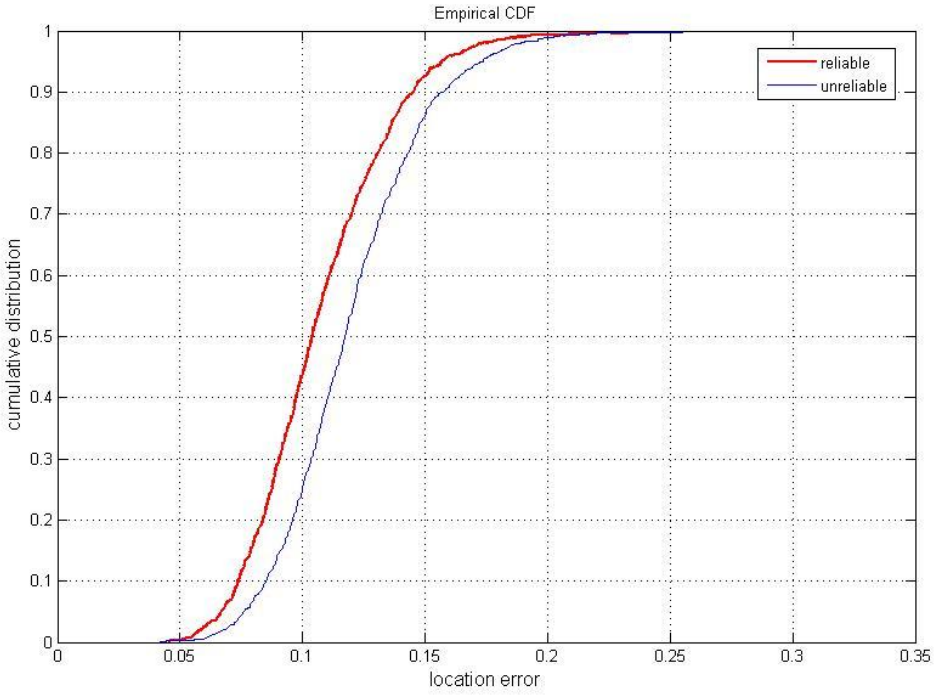

(b)

Figure 4.10 Comparison of CDF of location error for sequential pre-linear method in (a) 2-D (b) 3-D case

We can see that the reliable measurements (red line) upgrade the performance no matter in joint pre-linear method in Figure 4.8, parallel pre-linear method in Figure 4.9 and sequential pre-linear method in Figure 4.10. In addition, the positions of mobiles also affect the localization. The details will be given in Section 4.2.2.

4.2.2 Positions of Mobiles

In (3.22), (3.35) and (3.43), F_k , y_k include the position of mobiles in *k-th* iteration and it also effect the estimation of mobiles. The position of mobiles plays a role that the measurements are unreliable if two mobiles are far away between each other. Futher, the poor geometry location cause the uncertain virtual BSs and lead to degradation of localization. In Figure 4.11(a), we discuss the influnce on parallel and sequential methods. Mobiles are placed at [1 1], [9 1], [9 9], [1 9] (distance between mobiles is far and in poor geometry) and [3 3], [7 3], [7 7], [3 7] respectively. In 3-D case, the mobiles are placed at [1 1 1], [5 1 5],[5 5 1], [1 5 5] and [2 2 2], [4 2 4], [4 4 2], [2 4 4]. The simulation results are shown in the following figures.

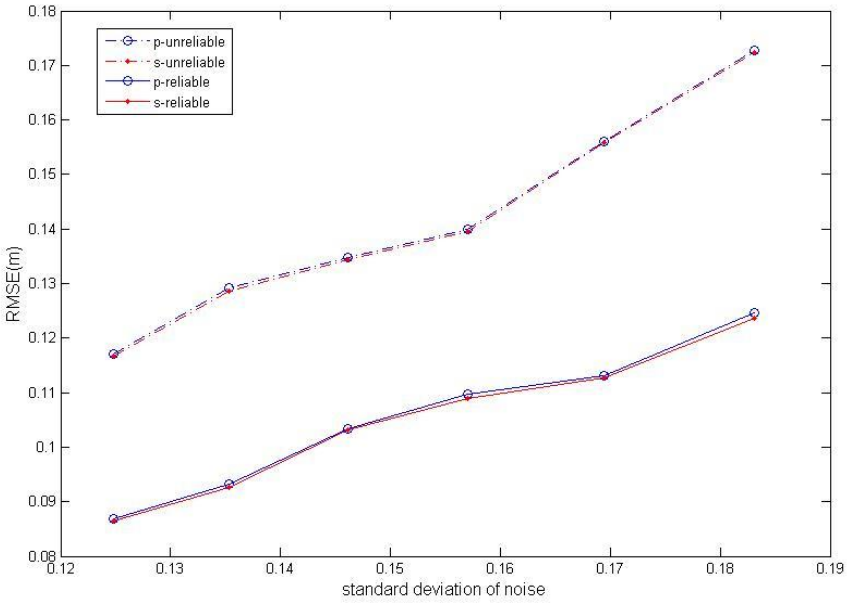

(a)

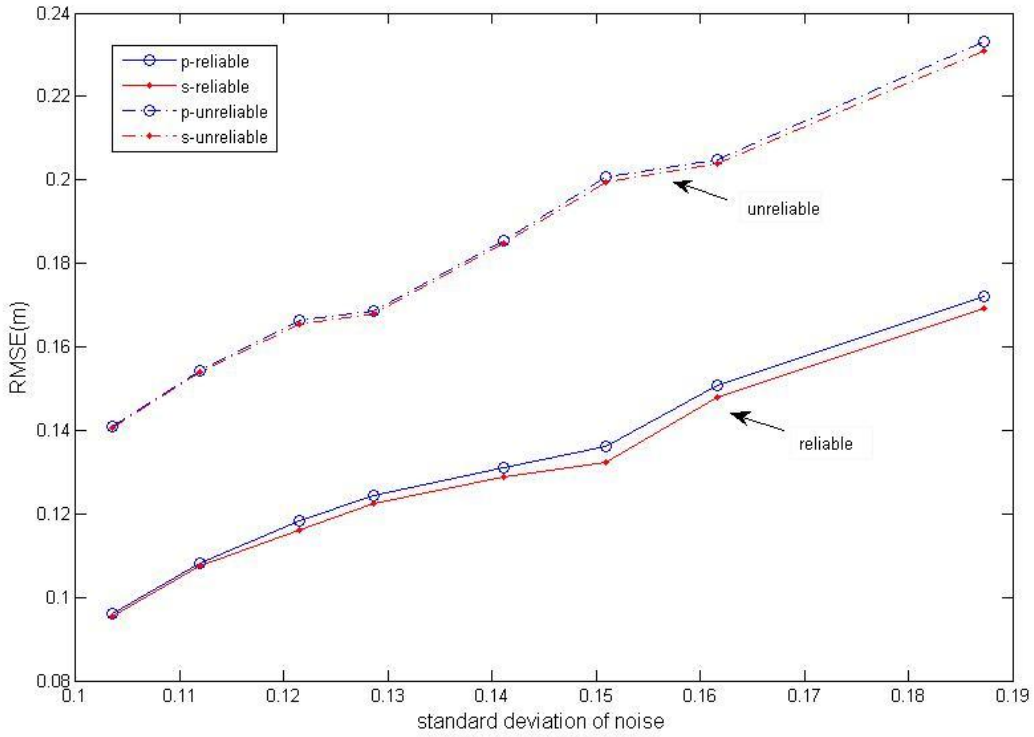

(b)

Figure 4.11 Influence of positions of mobiles on different noise variance in (a) 2-D (b) 3-D case

In parallel and sequential pre-linear method, the positions of uncertain virtual BSs are used in (3.29) and (3.37) respectively, and it can affect the performance. The RMSE of parallel and sequential pre-linear methods are shown in Figure 4.11. We can see that the performance is better if the positions are set closer and near in the middle of geometry. The influence of uncertainty of mobile will be modified based on mobile selection and weighting compensation in Section 4.3 and Section 4.4.

4.3 Effect on Target Mobile

In this Section, the target mobile selection schemes are considered. We want to modify the performance with the probable target mobile. In 2-D case, mobile *1* is selected at [2 2] and others are randomly selected in $2\times2(m)$ in the middle of geometry. Note that we select mobile*1* as target mobile in general case, and pick a mobile from all candidates as target mobile in target mobile selection scheme. In 3-D case, the procedures are identical with 2-D case. We select mobile *1* at [2 2 2], and others are in $3.5\times3.5\times3.5(m)$ in the middle of geometry.

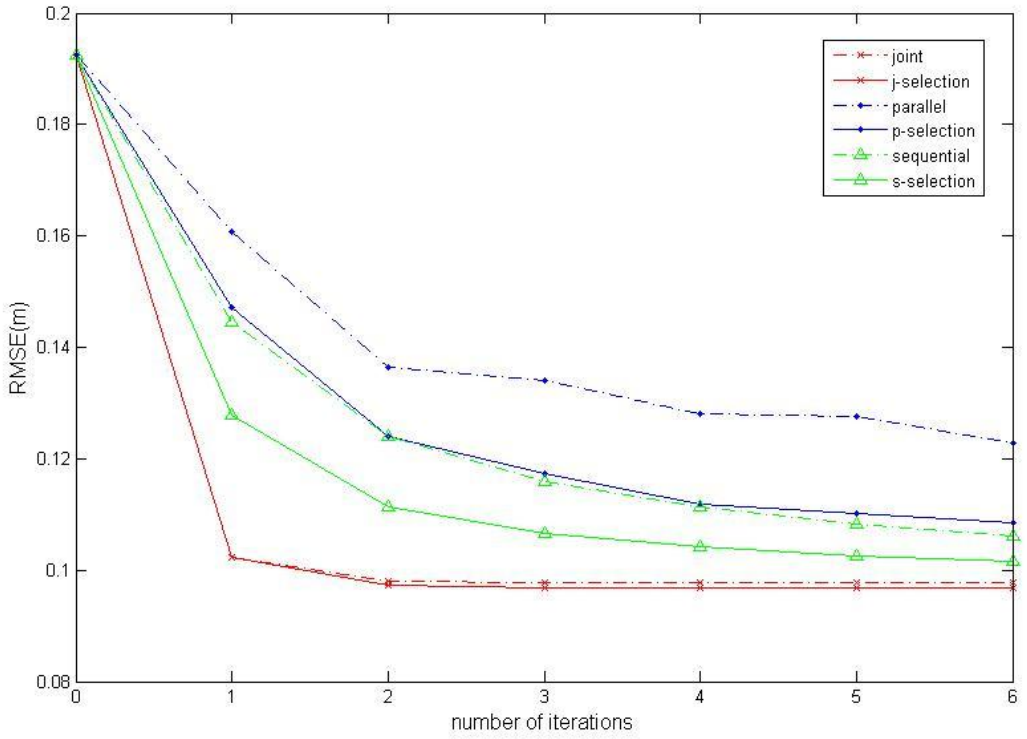

(a)

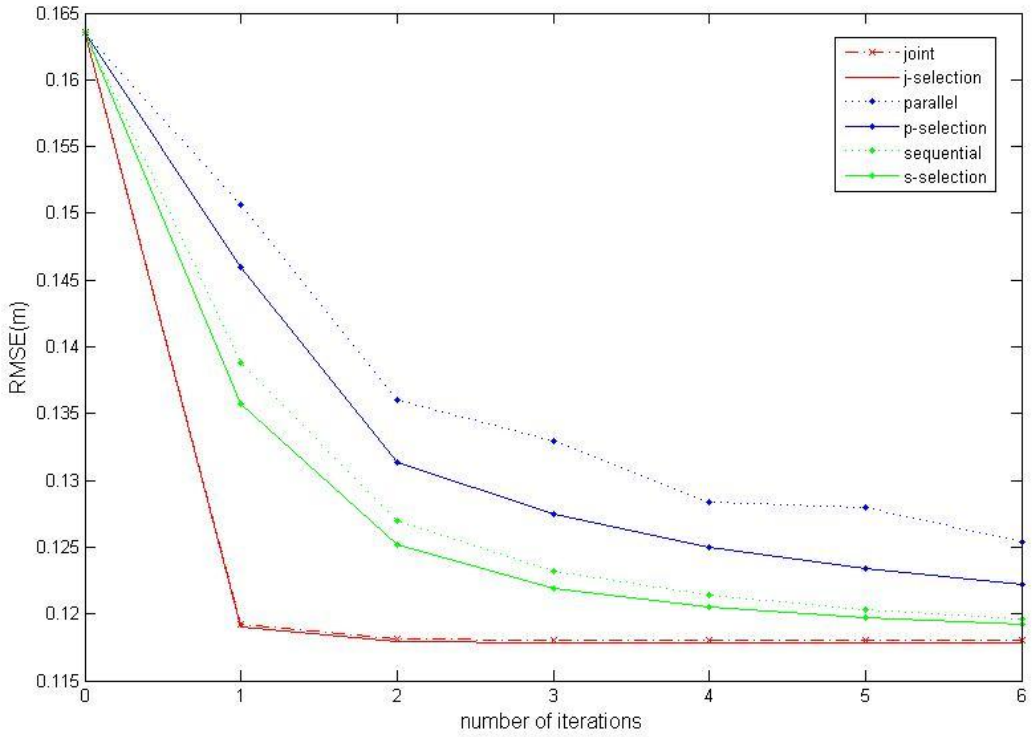

(b)

Figure 4.12 Influence of target mobile selection in (a)2-D (b) 3-D case

From Figure 4.12, we can see that the performance of mobile selection (solid line) is improved compared with the genaral case (dashed line), especially in parallel (blue) and sequential (green) pre-linear methods, while the joint method improves slightly. We infer that in joint method, the mapping function comes from the cooperation of all the auxiliary mobile, and the influence on target mobile is less than parallel and sequential methods..

4.4 Weighting Compensation

In this Section, the effect on weighting are discussed. Section 4.4.1 shows the poor initial value degrades the performance. The improvement on weighting of noise variance is shown in Section 4.4.2. In Section 4.4.3, weighting compensation on virtual BSs and target mobile upgrades the RMSE of localization.

4.4.1 Initial Value

It is known that a good initial value is important when the Taylor-series expansion is used to linearize the nonlinear function, or the Taylor higher order truncation error can not be neglected. Our pre-linear methods are based on GN method which applies Taylor-series expansion to non-linear range function. The following figure shows the effect when the poor initial value is used.

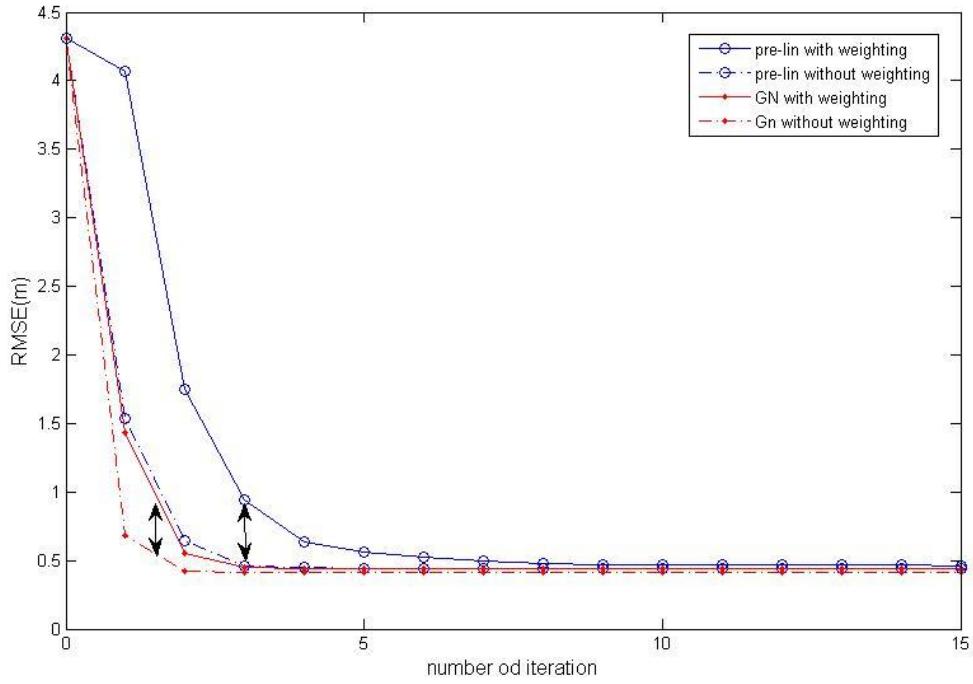

Figure 4.13 RMSE vs. iteration for a poor initial value

In Figure 4.13, the number of mobiles is equal to 2 and randomly located within $10\times10\times4(m)$ in $12\times12\times6(m)$ cube with four BSs at the corner like Figure 4.2. We give an initial value at [6 6 3] and [5 5 4]. Note that it is a special case of pre-linear methods in *M*=2 that there is only one way to generate the mapping function. We can see that in GN method (red line) and pre-linear method (blue line), the algorithm with variance of noise (solid line) can not improve the RMSE. The term $n_{ts,ij}$ in (3.6) dominate the total error, i.e., $n_{ts,ij} > n_{ij}$. In Section 4.4.2, a good initial value is used so that the noise dominates the total error.

4.4.2 Effect on Weighting of Noise Variance

Here, the statistics of noise variance σ_{ij} is considered in the following figures

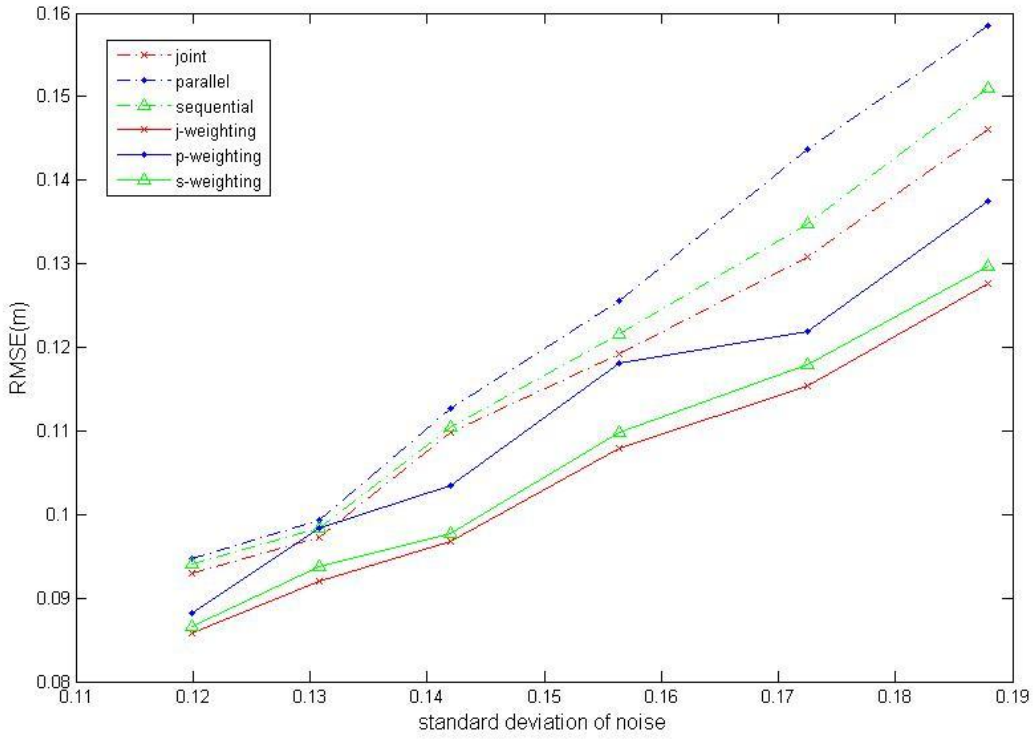

(a)

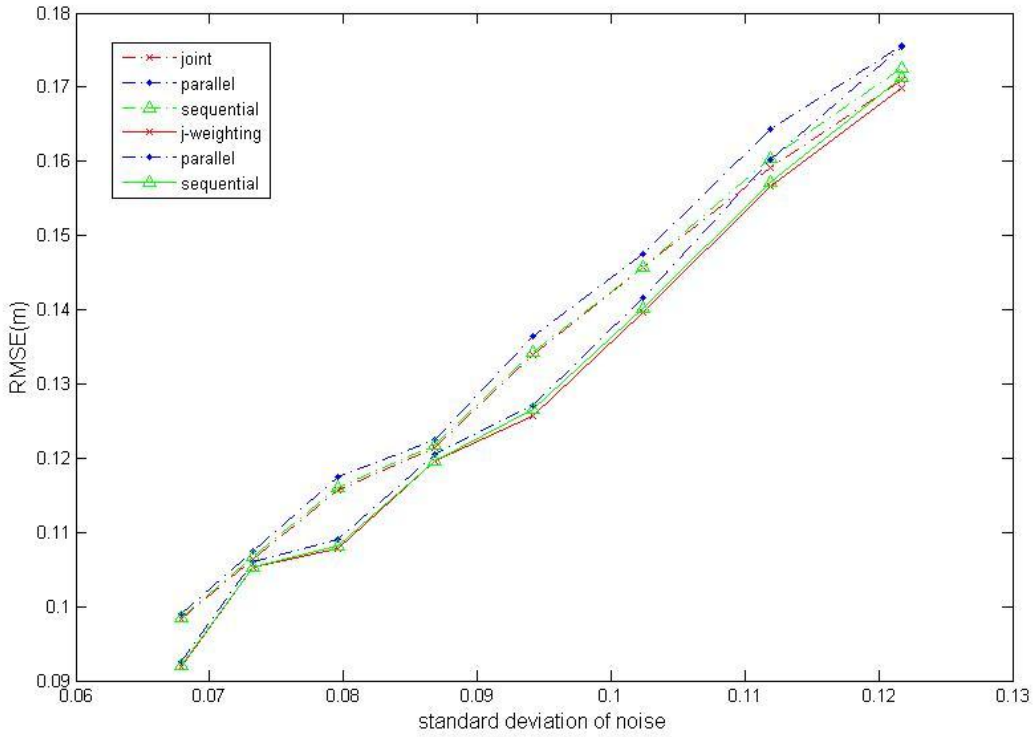

(b)

Figure 4.14 The effect on weighting of noise variance in (a) 2-D (b) 3-D case

We can see that RMSE is improved with the weighting of noise variance obviously in three pre-linear methods. Different from 4.4.1, the uncooperative LLS estimator offers a not bad initial value in this section. From Figure 4.14, we further know that the noise variance dominates the localization rather than the Taylor truncation error, i.e., $n_{ij} > n_{ts,ij}$.

4.4.3 Weighting Compensation

The compensation of uncertain position of virtual BSs and the target mobile in three pre-linear methods in (3.23), (3.36) and (3.44) are considered. The simulations are given in following figure.

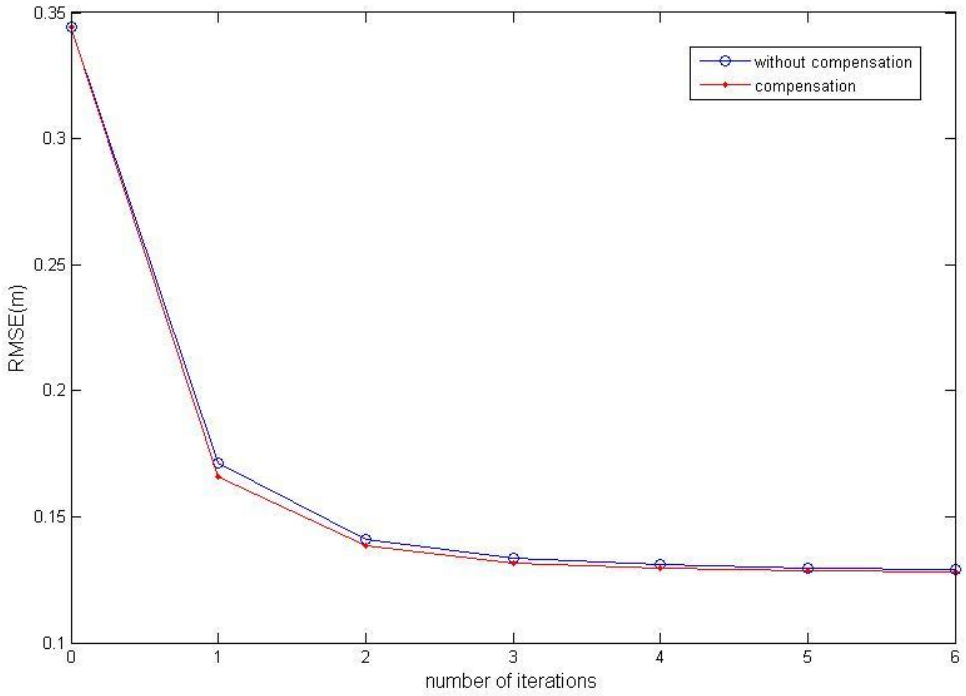

(a)

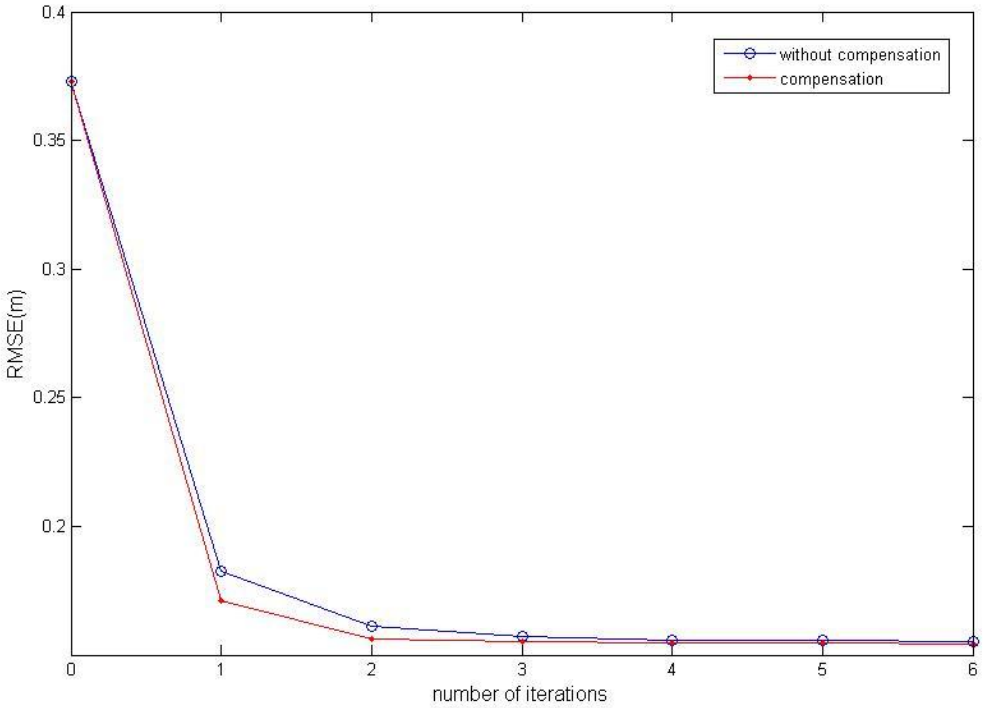

(b)

Figure 4.15 Weighting compensation on joint method in (a) 2-D (b) 3-D case

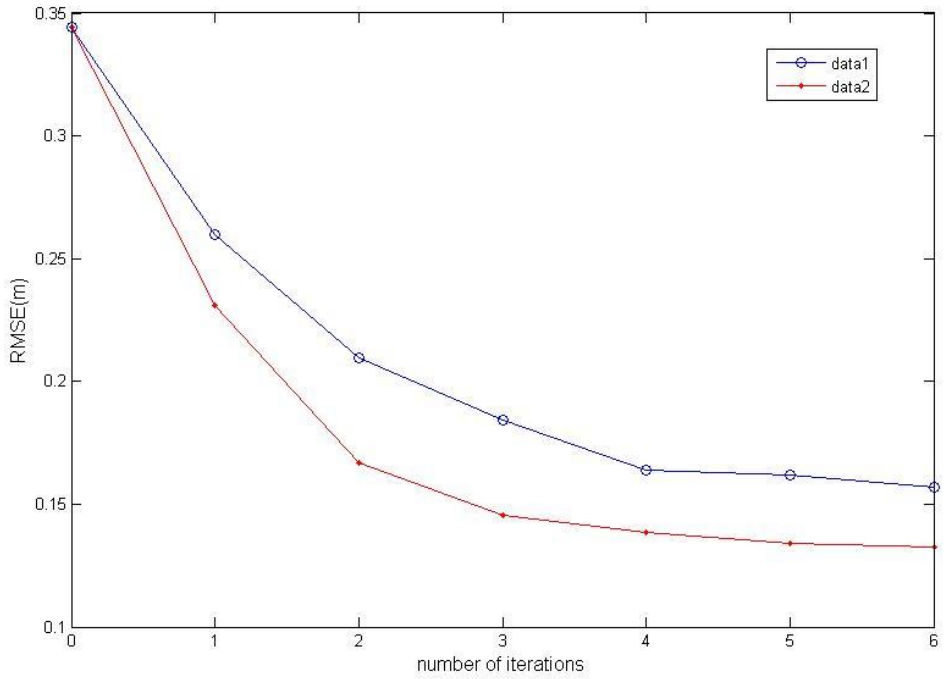

(a)

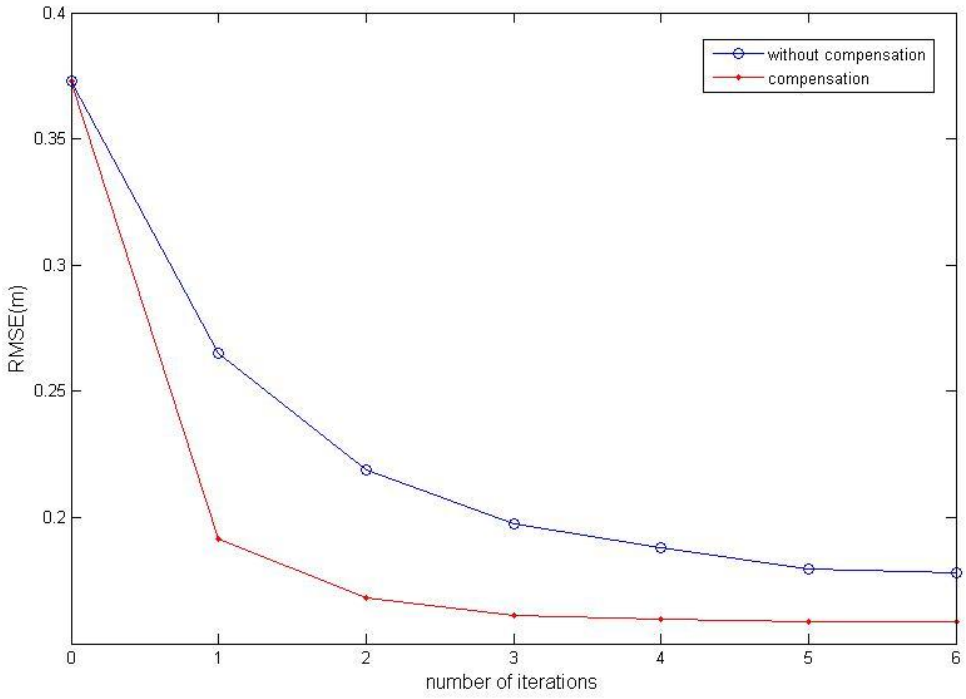

(b)

Figure 4.16 Weighting compensation on parallel method in (a) 2-D (b) 3-D case

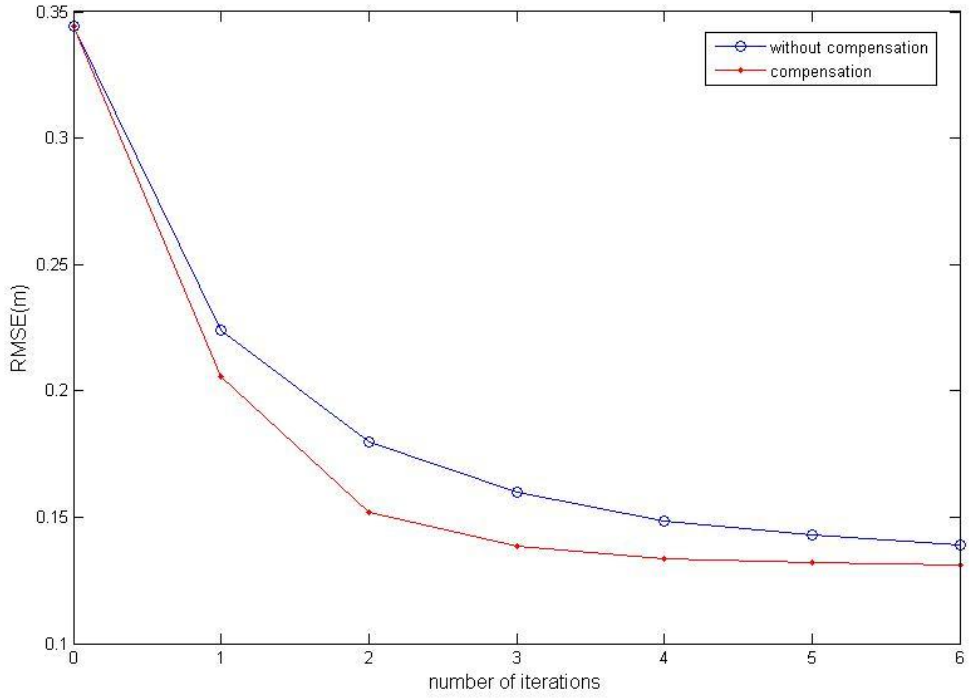

(a)

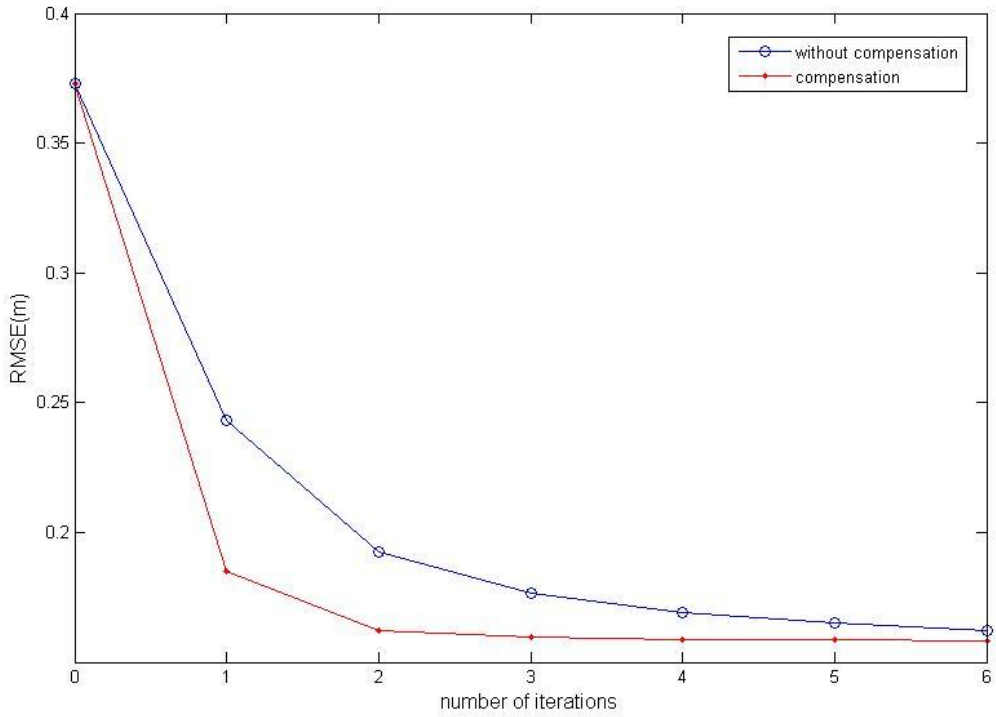

(b)

Figure 4.17 Weighting compensation on sequential method in (a) 2-D (b) 3-D case

From Figure 4.15 to 4.17, we can see that the compensation improves the RMSE. Note that there is an improvement for convergence in 3-D case. By iteration, the accurate positions of mobiles are obtained, the effect on location errors become smaller. The extra computation are $9(M-1)$ for joint method, $9(M-1)^2$ for parallel and sequential methods. In parallel and sequential methods , it is still less than joint GN method, we conclude that the compensation is useful in our proposed pre-linear methods.

Chapter 5
Conclusions and Future Works

In cooperative localization, three pre-linear methods based on distance measurement have been proposed to reduce the dimensions of unknown parameters in this thesis. Using the concept of linear mapping from target mobile to auxiliary mobiles, we expect that the complexity can be reduced. Compared with joint GN method, the total computation cost in each iteration saves roughly M^3 multiplication in parallel and sequential methods when the number of mobiles is increased. Simulation results validate that the RMSE of proposed methods are still comparable with joint GN method, but the total cost is reduced greatly. Simulations also show the influence on reliability of cooperative measurement; because the additional weighting compensation for uncertain position of mobiles not only improves the location accuracy, the convergence is also improved. Moreover, we can see that target mobile selection scheme enhances the RMSE. In a word, the contribution of this thesis is that we propose three low complexity pre-linear methods with good accuracy.

In fact, there exist lots of mapping relation that the mapping can be generated based on different localization requirement. Here, the linear mapping we proposed is based on the requirement for low complexity. Besides, the proposed methods can be also applied in NLOS environment. In the end, the theoretical analysis of proposed methods are another attractive issue to verify the performance.

Bibliography

[1] N. Patwari., J.N. Ash, S. Kyperountas, A.O. Hero, III, R.L. Moses, and N.S. Correal, "Locating the nodes: cooperative localization in wireless sensor networks," *IEEE Signal Processing Magazine*, Volume 22 , pp. 54 - 69 , 2005.

[2] N.A. Alsindi, B. Alavi, and K. Pahlavan, "Measurement and modeling of ultrawideband TOA-based ranging in indoor multipath environments," *IEEE Transactions on Vehicular Technology* Volume 58, pp. 1046 – 1058, 2009.

[3] A.N. Bishop, B. Fidan, B.D.O. Anderson, K. Dogancay; and P.N. Pathirana, "Optimal range-difference-based localization considering geometrical constraints," *IEEE Journal of Oceanic Engineering*, Vol. 33, pp. 289 – 301, 2008.

[4] M. Souden, S. Affes, and J. Benesty, "A two-stage approach to estimate the angles of arrival and the angular spreads of locally scattered sources," *IEEE Transactions on Signal Processing*, Volume 56, pp. 1968 – 1983, 2008.

[5] H. Ren, M. Meng, "Power adaptive localization algorithm for wireless sensor networks using particle filter," *IEEE Transactions on Vehicular Technology*, Volume 58, pp. 2498 – 2508, 2009.

[6] A. Broumandan, T. Lin, J. Nielsen, and G. Lachapelle, "Practical results of hybrid AOA/TDOA geo-location estimation in CDMA wireless networks," *2008. VTC 2008-Fall. IEEE 68th Vehicular Technology Conference*, pp. 1 – 5, 2008.

[7] W. Wang, J-Y Xiong, and Z-L Zhu, ''A new NLOS error mitigation algorithm in location estimation,'' *IEEE Transactions on Vehicular Technology,* Volume 54, pp. 2048 – 2053, Nov. 2005.

[8] N.A. Alsindi, B. Alavi, K. Pahlavan, and X. Ei, ''A novel cooperative localization algorithm for indoor sensor networks,'' *Personal, Indoor and Mobile Radio Communications,* IEEE, pp. 1-6, 2006.

[9] J. Yan, C. Tiberius, G. Bellusci and G. Janssen, ''Low complexity improvement on linear least-squares localization,'' *Communication System, IEEE Conference,* pp. 124-128, 2008.

[10] W. H. Foy, ''Position-location solutions by Taylor-series estimation,'' *Aerospace and Electronic System, IEEE Trans*, pp. 187-194, 1976.

[11] M.D. Gillette, H.F. Silverman, '' A linear closed-form algorithm for source localization from time-differences of arrival,'' *Signal Processing Letters, IEEE*, pp. 1-4, 2008.

[12] S. Wu, J. Li, and S. Liu, ''An improved reference selection method in linear least squares localization for LOS and NLOS,'' *Vehicular Technology, IEEE Conference*, pp. 1-5, 2011.

[13] J. Yan, C. Tiberius, G. Bellusci and G. Janssen, ''A framework for low complexity least-squares localization with high accuracy,'' *IEEE transactions on Signal Processing*, vol. 58, no. 9, pp. 4836-4847, 2010.

[14] F. Chan, H.C. So, and W.K. Ma, ''A novel subspace approach for cooperative localization in wireless sensor networks using range measurement,'' *IEEE Transactions on*

Signal Processing, volume: 57, pp 260-269, 2009.

[15] O. Abumansoor, A. Boukerche , ‘’A secure cooperative approach for Nonline-of-Sight location verification in VANET,’’ *IEEE Transactions on Vehicular Technology*, vol. 61, no. 1, 2012.

[16] P. Tarrio, A.M. Bernardos, J.A. Besada, and J.R. Casar, ‘’A new positioning technique for RSS-Based localization based on a weighting least squares estimator,’’ *Wireless Communication System, IEEE International Symposium*, pp. 633-637, 2008.

[17] Y. Zhang, Q. Cui, and X.F. Tao, ‘’Cooperative positioning for the converged networks,’’ *Vehicular Technology Conference, IEEE*, pp. 1-6, 2009.

[18] Timothy Sauer, ‘’Numerical analysis,’’ Boston: Pearson Addison Wesley, c2006.

[19] K. W. Cheung, H. C. So, W.-K. Ma, and Y. T. Chan, “Least squares algorithms for time-of-arrival-based mobile location,” *IEEE Trans. Signal Process.*, vol. 52, no. 4, pp. 1121–1128, Apr. 2004.

[20] A. O. Hero, III and D. Blatt, “Sensor network source localization via projection onto convex sets (POCS),” in *Proc. IEEE Int. Conf. Acoust., Speech, Signal Process.*, Mar. 2005, vol. 3, pp. 689–692.

[21] K.C. Ho, L.Yang, ‘’On the use of a calibration emitter for source localization in the presence of sensor position uncertainty,’’ *IEEE Trans on Signal Processing*, vol. 56, no. 12, Dec. 2008.

[22] H. V. Poor, ‘’An introduction to signal detection and estimation,’’ 2nd ed, New York: MA: Kluwer, 2000.

[23] I. Guvenc, S. Gezici, F. Watanable, and H. Inamura, ‘’Enhancements to Linear Least Squares Localization Through Reference Selection and ML Estimation,’’ *Wireless Communication and Networking Conference, IEEE*, 2008

[24] G. H. Golub and C.F. Van Loan, ‘’Matrix Computations, ‘’ 3rd.